

Chalcophile and platinum-group element distribution in the Ultramafic series of the Stillwater Complex, MT, USA—implications for processes enriching chromite layers in Os, Ir, Ru, and Rh

Sarah-Jane Barnes¹ · P. Pagé¹ · H. M. Prichard² · M. L. Zientek³ · P. C. Fisher²

Received: 13 June 2014 / Accepted: 25 March 2015 / Published online: 6 May 2015
© Springer-Verlag Berlin Heidelberg 2015

Abstract All of the rocks from the Ultramafic series of the Stillwater Complex are enriched in PGE relative to most mafic magmas. Furthermore, the chromite layers are particularly enriched in IPGE (Os, Ir, and Ru) and Rh. This enrichment appears to be a common characteristic of ultramafic rocks from many types of settings, layered intrusions, ophiolites, and zoned complexes. We have carried out a petrological, mineralogical, and geochemical study to assess how the enrichment occurred in the case of the Stillwater Complex and applied our results to the chromite layers of the Bushveld and Great Dyke complexes. The minerals that now host the PGE are laurite and fine-grained intergrowths of pentlandite, millerite, and chalcopyrite. The laurite occurs as inclusions in chromite, and mass balance calculations indicate that it hosts most of the Os, Ir, and Ru. The sulfide minerals occur both as inclusions in chromite and as interstitial grains. The sulfides host much of the Pd and Rh. The IPGE and Rh correlate with Cr but not with S or Se, indicating that these elements were not collected by a sulfide liquid. Palladium, Cu, and Se correlate with each other, but not with S. The low S/Se (<1500) of the

whole rock and magnetite rims around the sulfides indicate some S has been lost from the rocks. We conclude that to account for all observations, the IPGE and Rh were originally collected by chromite, and subsequently, small quantities of base metal sulfide liquid was added to the chromite layers from the overlying magma. The IPGE and Rh in the chromite diffused from the chromite into the base metal sulfides and converted some of the sulfides to laurite.

Keyword Platinum-group elements · Selenium · Chromite · Laurite · Ultramafic series · Stillwater Complex

Introduction

Most of the world's primary platinum-group element (PGE) resources are found within three layered intrusions, the Bushveld Complex of South Africa, the Stillwater Complex of MT, USA, and the Great Dyke of Zimbabwe (Naldrett 2011; Zientek 2012). The PGE deposits, in these intrusions, referred to as reefs, are narrow (1–3 m) PGE-rich (1–10 g/t) layers which occur within mafic to ultramafic rocks. In all three intrusions, there is 1–2 km of ultramafic rocks below the reefs. The means whereby the PGE come to be concentrated in the reefs is much debated. Some authors favor a strictly orthomagmatic model with saturation of the magma with a sulfide liquid at the level of the reefs, the PGE partition into the sulfides liquid, which is then collected on the magma pile to form a PGE-rich layer (Keays et al. 2012). Some authors suggest that the PGE were collected from the underlying cumulate pile by late magmatic fluids and precipitated in the reef layers (Boudreau and McCallum 1989; Hanley et al. 2008). Others suggest more complex models involving both processes (Godel and Barnes 2008).

Editorial handling: G. Beaudoin

Electronic supplementary material The online version of this article (doi:10.1007/s00126-015-0587-y) contains supplementary material, which is available to authorized users.

✉ Sarah-Jane Barnes
sjbarnes@uqac.ca

¹ Sciences de la Terre, Université du Québec à Chicoutimi, Chicoutimi G7H 2B1, Canada

² School of Earth and Ocean Sciences, Cardiff University, Cardiff CF10 3AT, UK

³ United States Geological Survey, Spokane Office, Spokane, WA, USA

In all three intrusions, there are numerous chromite layers in the rocks below the reefs. These chromite layers are known to be enriched in PGE (Naldrett et al. 2009; Scoon and Teigler 1994; von Gruenewaldt et al. 1986; Oberthür 2002; Zientek et al. 2002), and yet most of these layers contain <100 ppm S, which suggests that collection by a sulfide liquid will not suffice to explain the PGE enrichment (Barnes et al. 2009). Furthermore, in the case of the Bushveld and Great Dyke, the IPGE (Ir, Os, and Ru) and Rh are enriched more than Pt and Pd in most chromite layers. Thus, some other processes must be important in controlling the PGE in these rocks because collection by a sulfide liquid would be expected to enrich the layers in all the PGE. Two models have been proposed to account for the IPGE enrichment in the chromite layers. The first suggests that laurite, (RuOs)₂, co-crystallized with chromite from a sulfide-understaturated magma. The presence of laurite would enrich the rocks in Os, Ir, and Ru. The second model proposes that a sulfide liquid collected the PGE from the magma and that this liquid collected on the cumulate pile. Subsequently, late magmatic fluids partly dissolved the sulfides, removing S, Pd, and some Pt, leaving a residuum enriched in IPGE and Rh (Boudreau and McCallum 1989).

The discussion is partly hampered by the fact that studies combining petrographic, platinum-group mineral (PGM) observations with modern whole rock analyses are not available for rock types from all three intrusions, especially for the rocks outside the ore zones. At Stillwater, Keays et al. (2012) provide partial PGE data for the silicate rocks and Zientek et al. (2002) provided a summary of Pt, Pd, and Rh for some of the chromite layers, but there are no published complete PGE data sets for the chromite layers and host rocks. We have combined geologic and petrographic observations, platinum-group mineralogy, whole rock chalcophile, and PGE analyses for rocks from the Ultramafic series of the Stillwater Complex to consider which phases control the PGE concentrations in these rocks. We also compare these results with the equivalent data from the Bushveld Complex and the Great Dyke to consider models for the formation of the ultramafic sections of the intrusion.

We propose a new model based on the observation that the mantle-normalized pattern for chromite layers from Stillwater Complex is similar to the patterns from chromite grains in the marginal sills of the Bushveld Complex and to the patterns from chromite phenocrysts from volcanic rocks. This model proposes that prior to saturation of the magma in a sulfide liquid, the IPGE and some of the Rh partitioned into the chromite. Subsequently, small amounts of base metal sulfide liquid were added to the chromite layers. During cooling, chromite grains underwent sintering and incorporated some sulfides. As cooling continued Fe and Ni in the sulfide diffused into the chromite and the IPGE and Rh in the chromite diffused into the sulfide, transforming the base metal sulfide into laurite with remnant sulfides and a few PGM grains.

Materials and methods

Eighty samples were collected from two traverses, one in the Mountain View area and one in the Benbow area (Fig. 1). The samples were collected with the aim of sampling all of the petrographic and stratigraphic units present. The number of samples taken per unit depended on the thickness of the unit and the availability of outcrop. Forty-four samples are from the Ultramafic series and form the subject of this paper.

Polished thin sections were made of all the samples and were examined using a petrographic microscope. For the chromite-rich rocks, the samples were examined for PGM at Cardiff University using a Zeiss NTS (Cambridge Instruments) S360 scanning electron microscope and Oxford Instruments INCA ENERGY EDS system. No PGM study was carried out on the other rocks because the PGE concentrations are so low, <20 ppb, that it is unlikely that any PGM would be observed.

Sulfur, Se, and PGE were determined at LabMaTer, Université du Québec à Chicoutimi. Sulfur was determined by IR Horiba instrument using the method of Bédard et al. (2008). Selenium was determined by TCF-INAA using the method of Savard et al. (2006). Platinum-group elements and Au were determined by ICP-MS after collection by Ni-fire assay and Te coprecipitation following the method of Savard et al. (2010).

Determining major and trace elements in the chromite-rich rocks by conventional methods was challenging because of the difficulty in dissolving all of the chromite; therefore, most major and trace elements were determined using INAA at LabMaTer, following the method of Bédard and Barnes (2002). Ga and Ti could not be determined by INAA, and these two elements were determined by XRF on pressed powder pellets at Geolabs (Ontario Geological Survey). For the silicate rocks, major oxides were determined by X-ray fluorescence analysis and trace elements were determined by inductively coupled plasma mass spectrometry (ICP-MS) analysis at Geolabs.

A preliminary estimate of the PGE content of the base metal sulfides was made using samples from the B, G, and J chromite layers where the sulfide grains are large enough for analysis by laser ablation. The LabMaTer laser ablation system consists of an Agilent 7700× mass spectrometer with an Excimer 193 nm Resonetics Resolution M-50 laser ablation probe. Six samples, reference materials, and blanks were placed in the chamber together. The reference materials and blanks were run before and after each sample. The spectrum was collected for 30 s with the laser switch off to determine the baseline. Then, a spectrum was collected for 30 s using spot analyses and a beam size of 20 μm (the size of the beam was limited by the small size of the sulfide grains). The laser frequency was 15 Hz, and the power of 0.5 mJ/cm³. An argon–helium gas mix was used as carrier gas. The material was

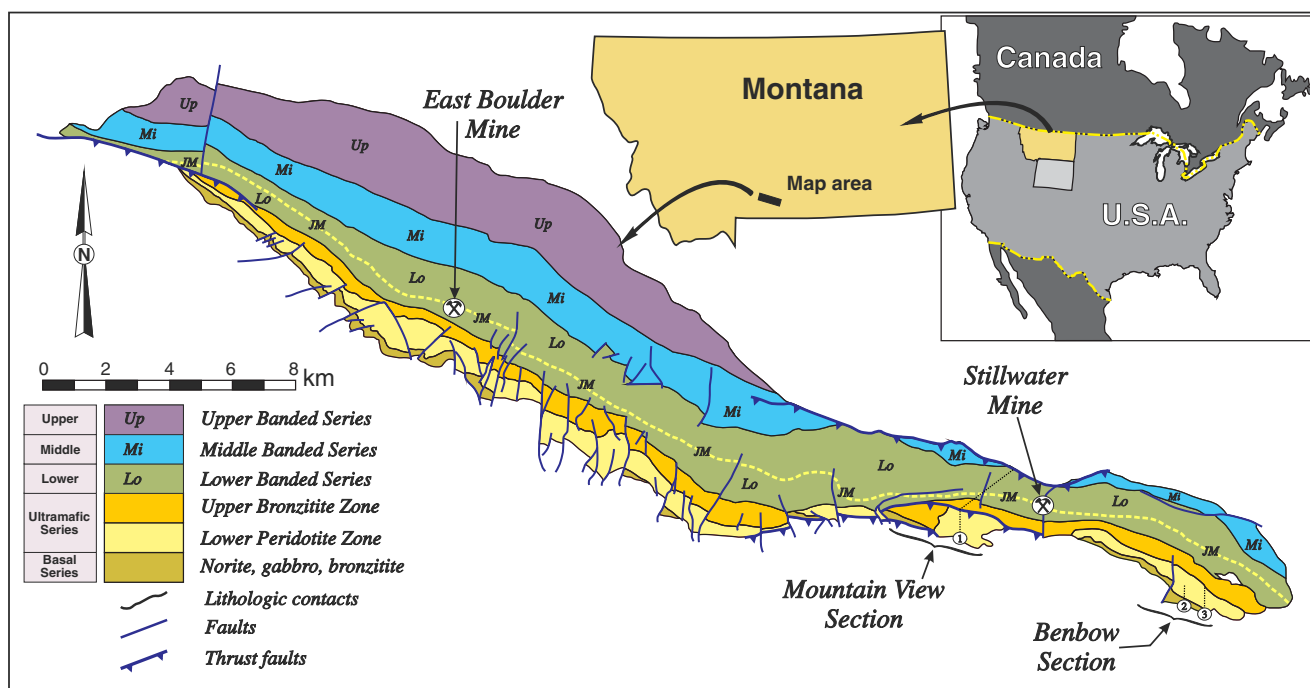


Fig. 1 Map of the Stillwater Complex showing the principle units and the location of the traverses sampled. Modified after Todd et al. (1982) and Zientek et al. (2002)

then analyzed using the mass spectrometer in time resolution mode using mass jumping and a dwell time of 10 ms/peak. The following isotopes were monitored: ^{29}Si , ^{33}S , ^{34}S , ^{53}Cr , ^{57}Fe , ^{59}Co , ^{61}Ni , ^{63}Cu , ^{66}Zn , ^{101}Ru , ^{103}Rh , ^{105}Pd , ^{108}Pd , ^{111}Cd , ^{189}Os , ^{191}Ir , ^{195}Pt , and ^{196}Pt . Data reduction was carried out using Iolite software. Internal standardization was based on ^{34}S . The certified reference material Po727, which is a synthetic FeS, doped with ~40 ppm of each PGE, and Au provided by the Memorial University of Newfoundland was used to calibrate for S, Fe, PGE, and Au. For the remaining elements, we used the certified reference material MASS-1, a ZnCuFeS pressed powder pellet provide by the US Geological Survey. The calibrations were monitored using the in-house reference materials JB-MSS5. The material JB-MSS5 is a synthetic FeS with 1 wt% Ni, 20–65 ppm PGE provided by Prof. Brennan of the University of Toronto. ^{101}Ru and ^{103}Rh were corrected for ^{61}Ni and ^{63}Cu interferences by using a Ni and Cu blanks and are equivalent to 1–2 ppm Ru and to 1–4 ppm Rh in the Stillwater sulfides. In order to avoid the ^{65}Cu interference on ^{105}Pd , ^{108}Pd was used to determine Pd. This peak was corrected for ^{108}Cd interference using ^{111}Cd and is equivalent to 0.2 to 1 ppm Pd in the Stillwater sulfides. All PGM inclusions were excluded from the spectra. Chrome and Si were used to eliminate analyses which included chromite or silicates.

Results for all reference materials and an estimation of precision are presented in Electronic Supplementary Materials (ESM) 1.

Geological setting

The Stillwater Complex, MT, USA (Fig. 1) is a layered intrusion that was emplaced into the Wyoming Archean Province at 2709 ± 1 Ma (Wall et al. 2010). The host rocks consist of a meta-sedimentary sequence which was intruded by a granitoid suite between 2730 and 2790 Ma (Wooden et al. 1991). Pressure estimates based on contact metamorphism (3.7 Kbars, Thomson 2008) and fluid inclusions (4.3–5.6 Kbars, Hanley et al. 2008) suggest a depth of emplacement of 12 to 16 km. The complex underwent lower greenschist facies metamorphism at approximately 1700 Ma (Page 1977) and was uplifted during the Cretaceous Laramide orogeny (Butler 1966). Most rocks still have an igneous assemblage, but some contain serpentine, chlorite, actinolite, and epidote as a result of the metamorphism. The complex is approximately 42 km long with a stratigraphic thickness of 5–6 km. The true size of the intrusion is unknown because the upper parts of the intrusion have been eroded away and its fault bounded at both ends.

A number of different terminologies have been used for the rock types at Stillwater (McCallum 2002). The most frequently used in recent years has been the cumulate terminology whereby the rocks are named based on the presence of the cumulate minerals present, e.g., olivine cumulate, which is abbreviated to oC. Whereas this terminology is useful to the specialist, its use tends to obscure the presence of the intercumulus minerals, and it also depends on interpretation as to whether a mineral is cumulate or not, and finally, it is not immediately obvious to

the general reader what the terms mean. For these reasons, we will use the IUGS terminology, which is based on the total modal mineralogy of the rocks. *ESM2* shows a correlation between the IUGS terms and the cumulate terminology in order that the reader may cross-reference to recent publications which have used cumulate terminology.

The complex has been divided into five series: the Basal, the Ultramafic and the Lower Banded, Middle Banded, and Upper Banded series (McCallum et al. 1980). The PGE deposit, known as the JM reef, occurs ~200 m above the contact between the Ultramafic and lower Banded series (Fig. 1). Our study concerns only rocks from the Ultramafic series; therefore, only these will be describe below. The reader is referred to Zientek et al. (2002) and McCallum (2002) for an overview of the other series.

The thickness of the Ultramafic series varies from 2000 m in the Mountain View area to 840 m in the western part of the complex. This variation is thought to reflect the original topography of the intrusion’s floor (McCallum 2002). The lower part of the Ultramafic series, known as the Peridotite zone, consists of a series of cyclic units of harzburgites overlain by olivine orthopyroxenites and orthopyroxenites. Cooper (1997), in a detailed study of the stratigraphy of the Peridotite zone, showed that the cyclic units can be grouped into six megacyclic units

which show unconformable relationships, possibly due to variations in the topography of the floor of the intrusion.

Within the peridotites, layers of semi-massive to massive chromite are present. The chromite-rich zones are labelled A to K from the base upwards (Fig. 2). In most cases, each chromite zone consists of a number of chromite-rich layers (commonly 2 layers) separated by chromite-bearing peridotite or pyroxenite. In many cases, the silicate rocks associated with the chromite layers have a pegmatoidal texture. The thickness of individual layers of chromite vary from 1 cm to 1 m, with the layers in the G and H chromite zones being the thickest (~1 m) and the layers of the I and J chromite zones being among the thinnest (1–3 cm). At all localities, where it was possible, each layer of the zone was sampled. In Fig. 2, the samples are plotted in order of relative position and not absolute height in order to space the samples out.

The upper part of the Ultramafic series is called the Bronzite zone. The division between the Peridotite and Bronzite zones is marked by the disappearance of cumulus olivine (McCallum et al. 1980; Zientek et al. 2002). The Bronzite zone is a thick homogenous unit consisting of orthopyroxenite. The first appearance of cumulate plagioclase marks the top of the Bronzite zone and the beginning of the Lower Banded series.

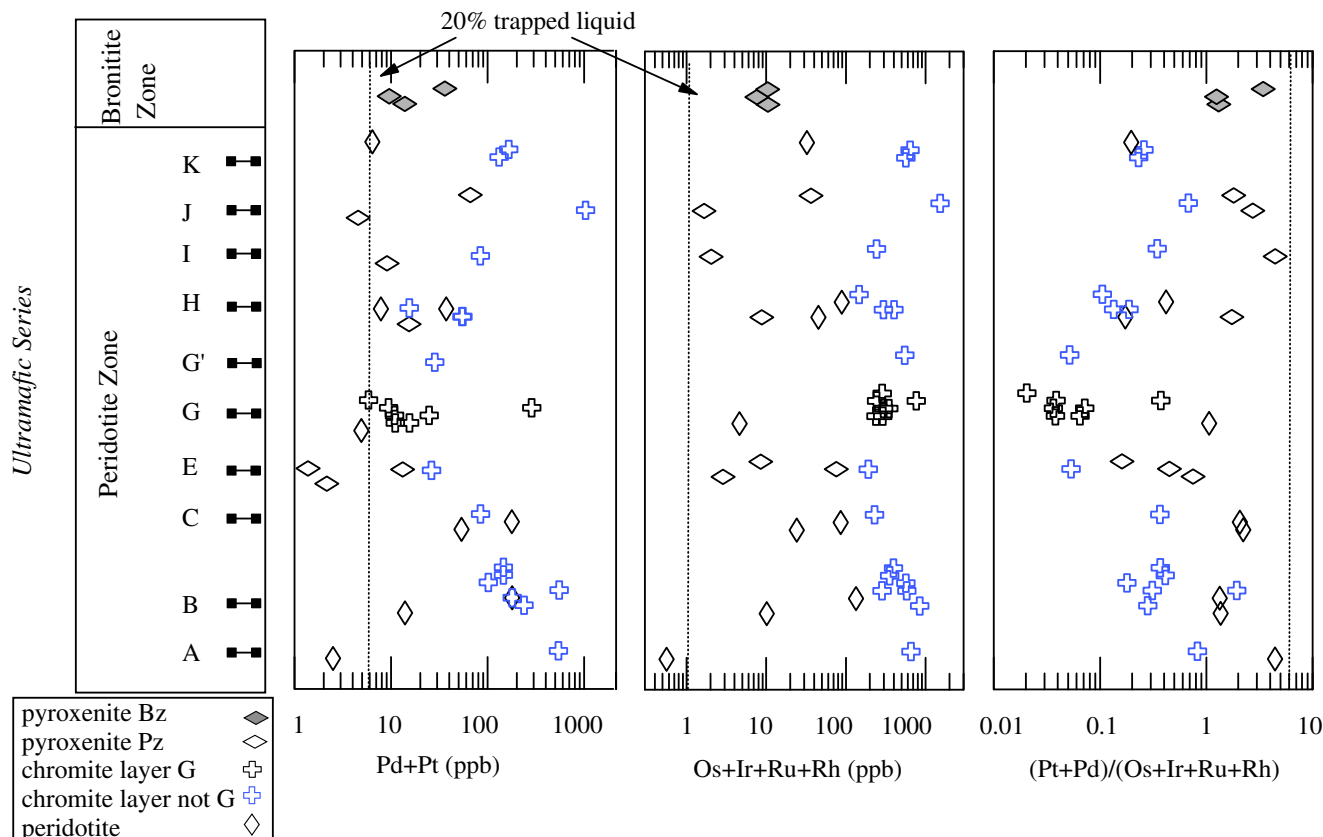
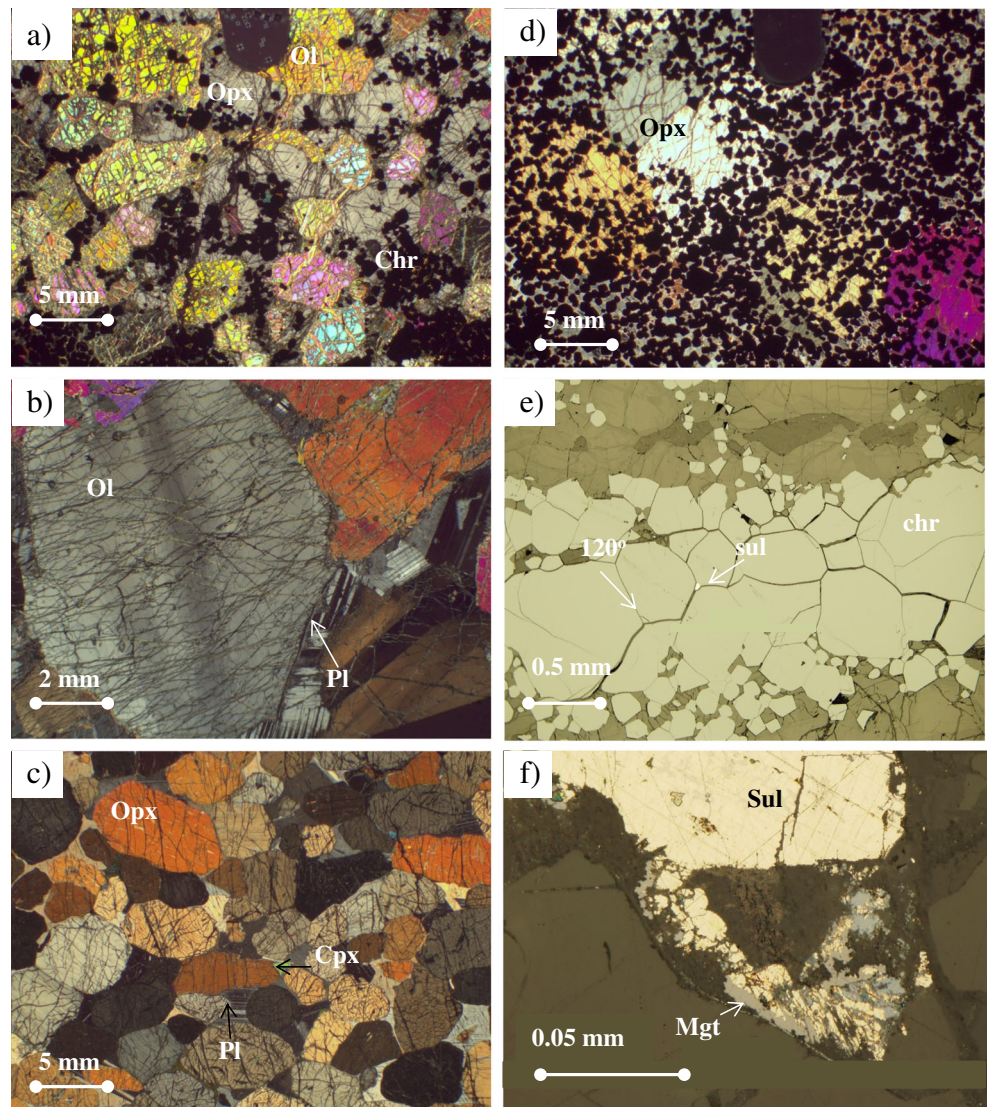


Fig. 2 Stratigraphy in the Mountain View area ■=chromite layer. Variations of Pt+Pd, Os+Ir+Ru+Rh and (Pt+Pd)/(Os+Ir+Ru+Rh) with stratigraphic position. Note that the absolute stratigraphic height was not

used. The samples are spaced relative to each other with the chromite layers spaced out evenly so as to clearly show the variations in the element concentrations

Fig. 3 Photomicrographs of the various rock types: **a** Poikilitic harzburgite showing olivine (*Ol*) and chromite (*chr*) chadocrysts in orthopyroxene (*Opx*) oikocrysts. **b** High temperature deformation twins in olivine and plagioclase (*Pl*). **c** Adcumulate orthopyroxenite showing euhedral orthopyroxene, with a few clinopyroxene (*Cpx*) rims and interstitial plagioclase. **d** Semi-massive chromite showing the euhedral shapes and small grain size. **e** Narrow massive chromite layer in orthopyroxenite showing contrast between chromite within the layer (large grain size and triple junctions with 120°) and disseminated chromite outside the layer. Note also the small sulfide at the triple junctions. **f** Base metal sulfides partially altered to magnetite



Results

Petrography

The most common form of harzburgite is the poikilitic harzburgite (Fig. 3a). It consists of ~60–70 % (approximate modal proportions based on thin section observations) olivine chadocrysts (3–10 mm) surrounded by orthopyroxene oikocrysts (10–50 mm), which make up ~10–30 % of the rock. Anhedral plagioclase grains (0.5–2 mm) are also present as the most common (2–10 %) interstitial mineral. Both the plagioclase and olivine show high temperature deformation twins (Fig. 3b). Small (0.2–1 mm) euhedral chromite grains are present both as inclusions within the olivine and orthopyroxene, and it also occurs between the olivine and orthopyroxene grains (Fig. 3a). The amount of chromite varies from 1 to 5 %. Trace amounts of phlogopite are present at the margin of some orthopyroxene grains and around some

chromite grains. In some samples, olivine has been partly altered to serpentine and magnetite, orthopyroxene has been altered to talc, and plagioclase has been replaced by chlorite and zoisite.

In many cyclic units, the poikilitic harzburgite grades into upwards into granular harzburgite and then olivine orthopyroxenite. Both of these rock types have meso to adcumulate textures and consist of (10–60 %) subhedral olivine (3–5 mm) and (30–70 %) anhedral to subhedral orthopyroxene (4–8 mm). Interstitial to the olivine and orthopyroxene are (2–5 %) anhedral plagioclase grains (0.5 to 2 mm). A few small (0.5 mm) euhedral chromite grains are also present. Phlogopite (0.5–1 mm) occurs surrounding a few chromite and orthopyroxene grains. As in the case of the poikilitic harzburgite in some samples, serpentine, talc, chlorite, and zoisite are present replacing the parts of the primary minerals.

The olivine orthopyroxenite grades into orthopyroxenite in some cyclic units, and most of the Bronzite zone is made up

of orthopyroxenite (Fig. 3c). The orthopyroxenites consist of mesocumulates of subhedral (4–7 mm) orthopyroxene (85 %) with interstitial anhedral (1–2 mm) plagioclase (5–10 %) and (0.2–0.5 mm) clinopyroxene ((1–2 %). A few ($<<1$ %) small (0.2–0.4 mm) chromite grains are present. Phlogopite occurs on the edge of some orthopyroxene grains. Most of the minerals are unaltered, but there are some fractures filled with fine-grained alteration minerals.

Chromite layers consist of >50 % chromite and, in some cases, up to 90 %. In the semi-massive layers where most of the chromite grains do not quite touch, the grains are euhedral and small (0.2–0.5 mm) (Fig. 3d). In contrast to the massive layers, many of the chromite grains are larger (1–2 mm), anhedral, and have 120° triple junctions, suggesting that they grew post-cumulus (Fig. 3e). The interstitial minerals in most of the chromite layers are subhedral olivine and oikocryts of orthopyroxene. Exceptions to this are the E and J chromite layers where the interstitial mineral is predominantly subhedral orthopyroxene (Fig. 3d).

Sulfide and platinum-group element minerals

The abundance of base metals sulfide minerals (BMS) in most samples is very low ($<<0.1$ %). The BMS occur as very small irregular patches, 0.01–0.1 mm in size which are present both as interstitial aggregates of grains and as inclusions within the chromite grains. Pentlandite was the BMS most frequently found followed by chalcopyrite; however, in some samples, bornite and millerite are present. Many of the sulfide patches are surrounded by magnetite rims and have magnetite veins cross-cutting them (Fig. 3f). The presence of these veins together with the presence of bornite and millerite suggest that the sulfides have been altered and that the samples may have lost S.

Pentlandite and millerite have been shown to contain high levels of PGE in the Lac des Iles, Bushveld, and Great Dyke Complexes (Djon and Barnes 2012; Smith et al. 2014; Junge

et al. 2014; Oberthür 2002). Therefore, analyses of the sulfide patches in layers B, G, and J that are large enough for analyses by laser ablation mass spectrometry has been carried out. On average, the sulfide patches were Ni-rich and contained PGE at the 20 to 300 ppm level (ESM3).

The PGE content of most of the silicate rocks is very low (<20 ppb); therefore, the probability of observing PGM in the polished section was considered too low to justify a PGM study. However, the chromite-rich rocks contain IPGE and Rh concentrations greater than 100 ppb, and thus, polished sections of these were examined for PGM. As in the case of the BMS, the PGM occur both as inclusions in the chromite and as interstitial minerals. The PGM assemblages in these two settings differ, with the inclusion PGM consisting predominantly of laurite, and the interstitial PGM consisting predominantly of Pd-PGM followed by Pt-PGM (Cooper et al. 2005; Prichard et al. 2014).

Most inclusions consist largely of laurite (Fig. 4a). The laurite grains range in size from 1×1 to 9×18 μm , but most are in the 1–5 μm range (ESM4, Fig. 5). In many cases, the inclusions consist only of laurite (Figs. 4b and 5a). However, in some cases, the laurite occurs together with silicates or rutile (Figs. 4b and 5b) or with base metal sulfides and other PGM (Figs. 4b and 5c, d ESM4).

Page (1971) provides sketches of two laurite inclusions in chromite from the G and H layers, and these are similar in shape and size to the laurites we observed. Talkington and Lipin (1986) have described laurites from the A, C, E, G, J, and K layers. Due to the limitations of the analytical methods of the time, they choose not to report individual analyses but rather reported the range in Ru# ($[\text{Ru}]/[\text{Ru}+\text{Os}+\text{Ir}]$) as 0.83 to 0.92 and mention that the laurites contain variable amounts of Rh from 0 to 1.8 wt%. Our laurite analyses show a similar range in Ru# (0.85 to 0.92), but a wider range in Rh values (less than detection level to 3 wt%, ESM 6). Talkington and Lipin (1986) observed that there was no correlation between the stratigraphy and the Ru# of the laurite. In contrast in our

Fig. 4 **a** Pie chart of PGM in the inclusions showing that laurite is the most common PGM in the inclusions. **b** Pie chart of the mineral assemblages in the inclusions

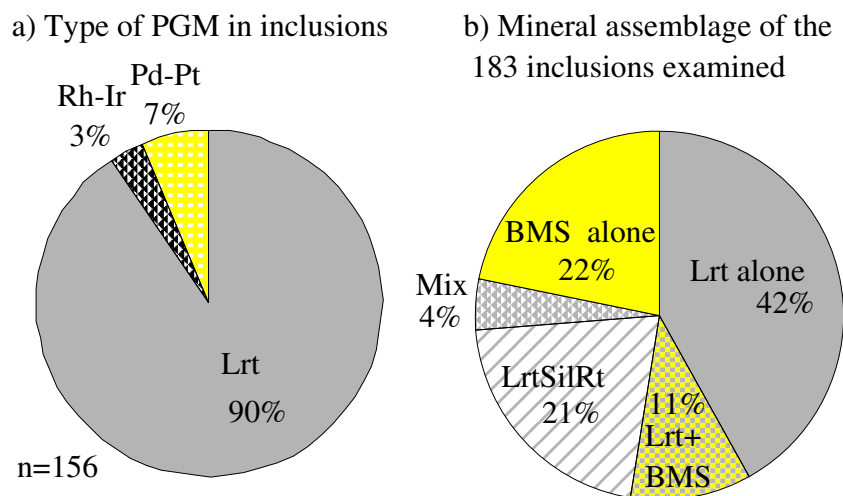
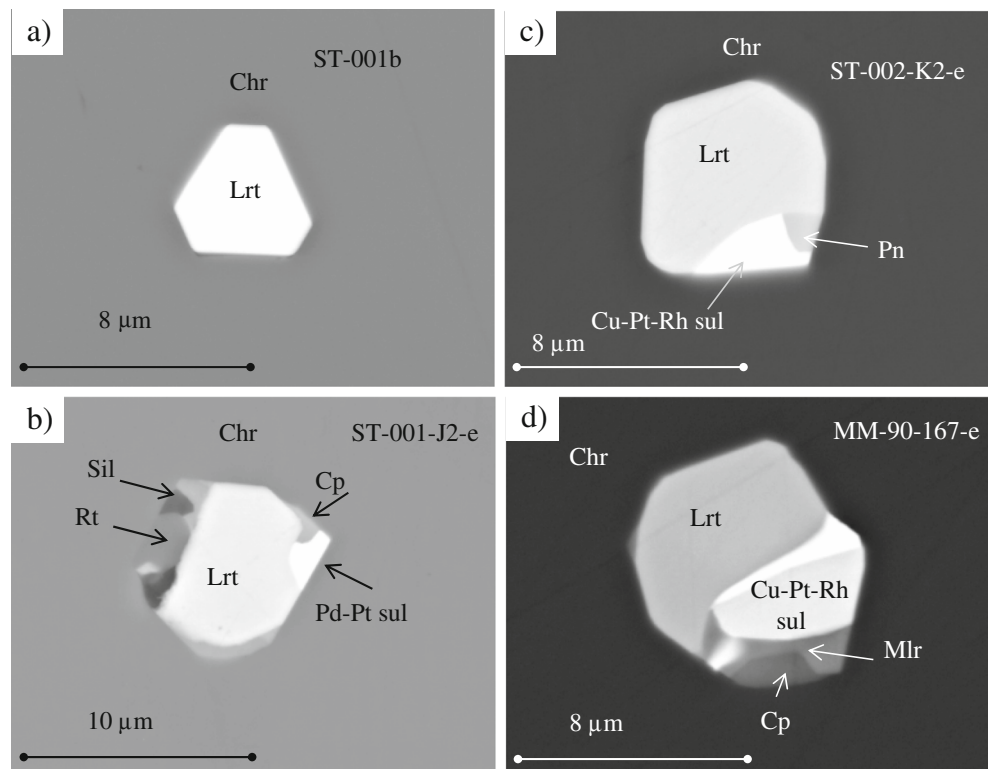


Fig. 5 Back scatter electron images of platinum-group mineral inclusions in chromite and their textures: **a** The most common type euhedral laurite (*Lrt*) in chromite (*Chr*). **b** Complex intergrowth of laurite, Pd–Pt sulfide, chalcopyrite (*Cp*), silicate (*Sil*), and rutile (*Rt*). **c** Intergrowth of laurite, malanite (Cu–Pt–Rh sul), and pentlandite (*Pn*). **d** Intergrowth of laurite, malanite, chalcopyrite, and millerite (*Mlr*)

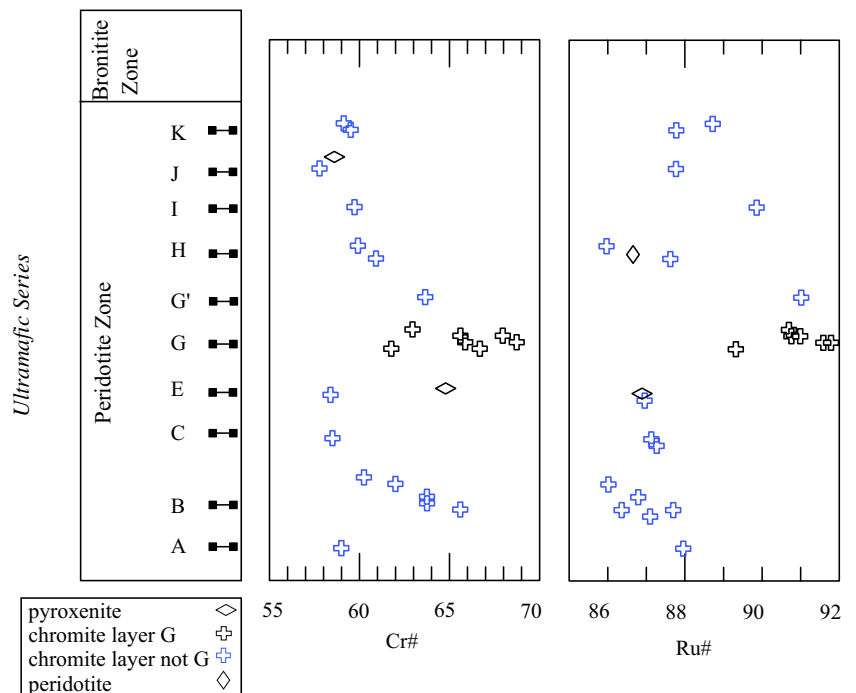


data set the Ru# of the laurites from the G-chromite layers are higher (0.9–0.92) than those from the other layers (Fig. 6, ESM 5). Interestingly, the chromites from the G layers also have higher Cr# than the other chromite layers (Fig. 6).

The composition of Stillwater laurite falls in the middle of range of laurites compositions from chromite layers in other layered intrusions (Fig. 7). The laurites from the Kemi

intrusion have lower Ru atoms per formula unit (afu). The laurites from the Bushveld, Bird River, and Compo Formso intrusions show a wider range in Ru afu (0.75 to 0.97 versus 0.85 to 0.93 for the Stillwater). The Os/Ir ratios are generally similar for laurites from all the intrusions (1–3), but there is a population of laurites from the Bushveld that have higher Os/Ir afu for a given Ru afu.

Fig. 6 Variations in Ru# of laurite and Cr# of chromite with stratigraphy across the Ultramafic series. Note that the Ru# of laurite and Cr# of chromite are highest in the G layer chromites, possibly indicating a new injection of magma at this level



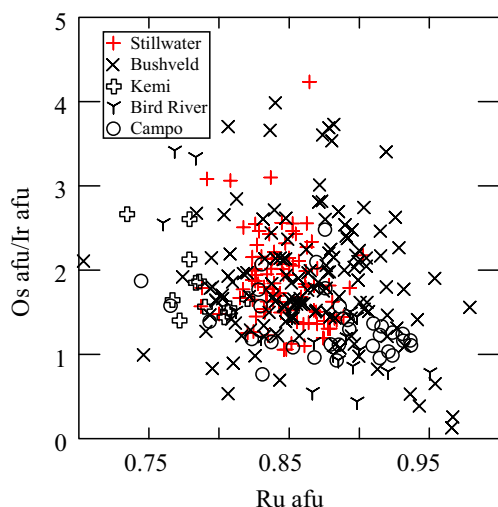


Fig. 7 Comparison of laurite compositions from Stillwater chromite layers with laurites from other layered intrusions. Data from Garuti et al. (2007); Gomostayev et al. (2000), Maier et al. (1999), and Ohnenstetter et al. (1986). Note the narrow range covered by the Stillwater laurites

The precise nature of most of the other PGM present in the inclusions is difficult to determine as they were mostly too small (0.1–2 μm) to obtain quantitative analyses. There is a CuPtRh(+/-Ir)S sulfide, which based on the two analyses we obtained, is probably a Rh-rich malanite (ESM 5). There are a few grains of PdPt sulfides and RhIr sulfides and one grain rich in Pt (Fig. 4b, ESM 4). In the majority of cases, some chalcopyrite, pentlandite, or millerite are present with these PGM (Fig. 5b–d, ESM 4). Page (1971) shows sketches of two inclusions from the H and G chromite grains which contain Pt alloy grains 5–10 μm in size in association with base metal sulfides and silicates.

The interstitial PGM from our samples of layers A, B, and J are predominantly present as tiny grains <1 μm in diameter associated with the interstitial BMS and consist mainly of sperrylite, platarsite, PtPd tellurides, a PdPb mineral, and CuPtFe alloy (Prichard et al. 2014). Cooper et al. (2005) report a similar assemblage in their observations of the interstitial PGM from the A, B, G, H, J, and K chromite layers.

Whole rock geochemistry

Zientek et al. (2002) reported that A and B chromite layers are enriched in Pt and Pd with values in the 300 to 3000 ppb range for (Pt+Pd), whereas the G and H chromite layers have much lower concentrations (10 to 40 ppb). Our data also show enrichment in the A and B and depletion in the G and H layers (Fig. 2, ESM 6). In addition, we can now state that most of the other chromite layers C, I, K, and J show moderate to substantial enrichment in Pt and Pd (100 to 1000 ppb). In contrast, the E and G' chromite layers and the silicate rocks contain low levels of Pt+Pd (1 to 30 ppb).

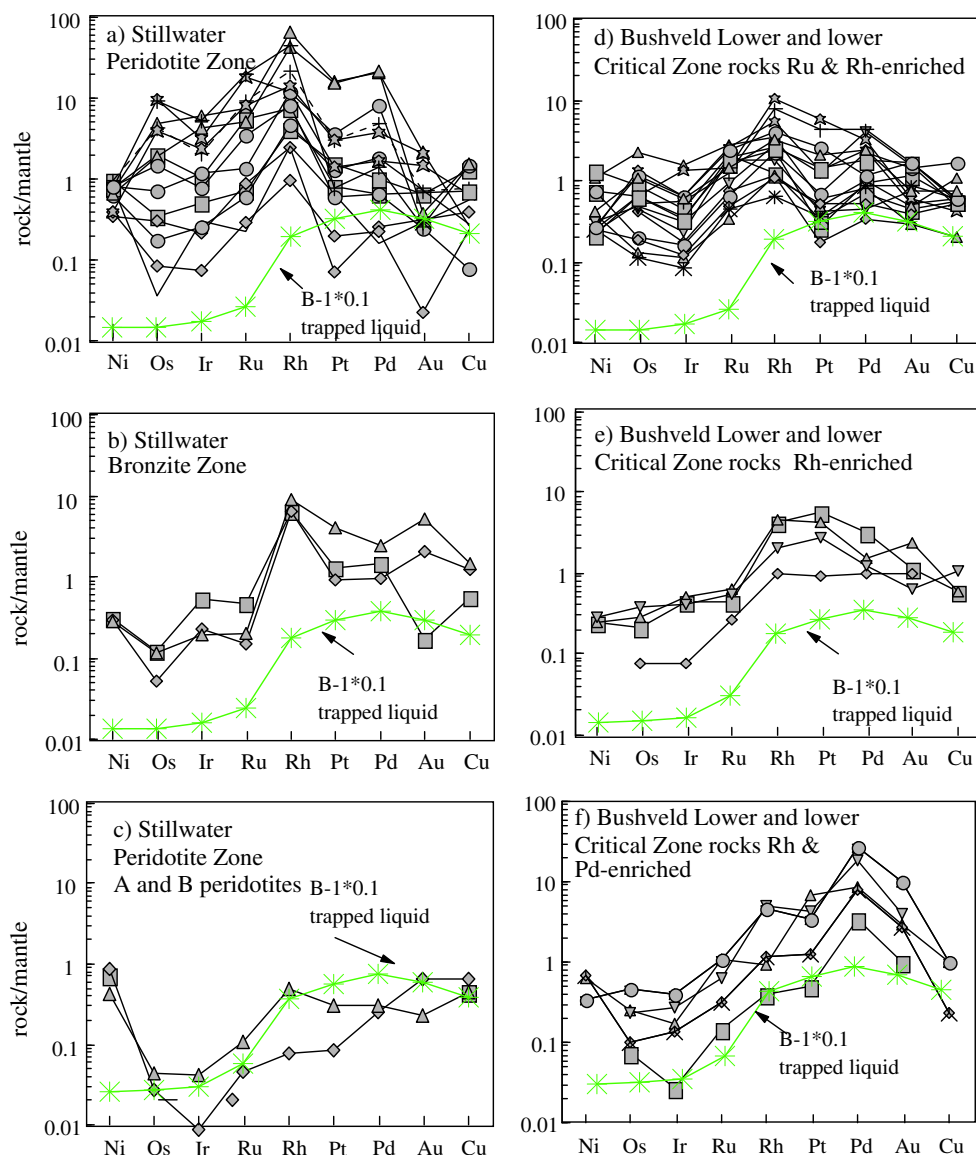
The IPGE (Os, Ir, and Ru) and Rh contents of the rocks vary from 0.1 to 1000 ppb, and there is no relationship between stratigraphic position and IPGE (Os, Ir, and Ru) or the Rh content of the rocks (Fig. 2, ESM 6). However, there is a clear difference in the IPGE and Rh contents of the chromite layers and the silicate rocks. The chromite layers are much richer in IPGE and Rh at 100 to 1000 ppb than the silicate rocks at 0.1 to 100 ppb (plus vs diamond symbols in Fig. 2).

Understanding how some rocks come to be enriched in PGE requires that one understand which phase(s) collected the PGE in the samples. One way to investigate this is to compare both the concentrations of PGE present and their inter-element ratios by using mantle-normalized metal patterns. If no phase has collected the PGE, then the PGE in the rock would essentially be present in the trapped liquid fraction and the whole rock mantle-normalized metal patterns should resemble that of a silicate liquid, but at lower level because of the dilution effect of the cumulate phases. Differences in patterns from the trapped liquid patterns require that some phase has collected or redistributed the PGE. Unfortunately, at Stillwater, the rocks that are thought to represent the primary magma, Mg-rich norite, have interacted with the country rock and contain percent levels of base metal sulfides (Zientek et al. 1986), making them unsuitable to estimate the PGE contents of the initial magma. In the following presentation, we have used the composition of the Bushveld marginal rocks as being representative of the magma (Barnes et al. 2010). We believe this assumption to be reasonable because the major element content of the mafic norite and the B-1 Bushveld magma are similar and because the Bushveld B-1 magma is similar in composition to primary mantle magmas with respect to PGE (Barnes et al. 2010). An exception to this observation is that the Bushveld marginal rocks contain slightly more Pt than most primary magmas (15–22 ppb vs 5 to 15 ppb).

The harzburgites and pyroxenites of the Peridotite and Bronzite zones have mantle-normalized metal patterns in the 0.1 to 10 range (Fig. 8a–c). There are two types of mantle patterns. A few samples of peridotites from the A and B units have patterns that resemble those of primary mafic magmas with an increase in PGE from Os to Pd and Pd/Ir ratios in the 10 to 30 range (Fig. 8a). These patterns show a regular increase from Os to Pt but are approximately an order of magnitude lower than that of a primitive magma represented here by the primary Bushveld magma. The peridotites are enriched in Ni, which is probably due to the collection of Ni by olivine in these rocks. Assuming that the rocks contain approximately 10 % trapped liquid fraction (consistent with the petrographic observations that the interstitial material represents 10–15 % of the assemblage), then the metal concentrations in these samples may be accounted for by considering them to be present in the trapped liquid fraction.

Most of the peridotite and pyroxenite samples have the patterns that are flat with Pd/Ir of approximately 2 and with

Fig. 8 Whole rock mantle-normalized metal patterns for the silicate rocks of the Stillwater and Bushveld Complexes. The trapped liquid fraction pattern (asterisk) is based on the B-1 magma of the Bushveld and assumes 10 % trapped liquid fraction. Bushveld data from Barnes et al. (2010) and Maier et al. (2013)



Ni and Cu approximately in line with the PGE (Fig. 8b, c). However, the pattern is not entirely flat due the presence of positive Rh anomalies (Fig. 8b, c). The samples from the Bronzite zone (Fig. 8c) show larger Rh anomalies than those from the Peridotite zone (Fig. 8b) because the Bronzite zone samples have lower IPGE (Os, Ir, and Ru) contents. Assuming that the rocks contained 10 to 20 % trapped liquid fraction, the Au and Cu content could be accommodated in this. Most samples show enrichments of Pt and Pd of up to an order of magnitude. For the IPGE and Rh, the enrichment relative to the primitive magma is even more marked with samples being enriched by one to three orders of magnitude (Fig. 8b, c).

The peridotites and pyroxenites from the Lower and lower Critical zones of Bushveld Complex show a similar range in patterns. Most samples have flat patterns apart from the Rh anomaly (Fig. 8d). A few samples have patterns similar to the Stillwater Bronzite zone, i.e., samples with a large Rh

anomaly due to the depletion in IPGE (Fig. 8e). Finally, there are a small group of samples from the Bushveld with patterns that show a continuous increase from Os to Pd (Fig. 8f). We did not observe this type of pattern at all in the Stillwater samples. We are not aware of data for peridotites and pyroxenites from the Great Dyke and thus cannot make a comparison for these rocks.

All of the Stillwater chromite layers are very strongly enriched in IPGE and Rh at 10 to 200 times mantle range (Fig. 9a, b) whereas Ni and Cu are in the 0.1 to 1 range; thus, all the patterns have arched shapes, characteristic of PGE reefs (Barnes et al. 1988). In most of the chromite layers, the mantle-normalized Pt, Pd, and Au values decrease slightly relative to Rh and are 10 to 100 times the mantle (Fig. 9). The G-chromite layer samples have slightly different patterns to the other chromite layers in that whereas they have similar shapes and levels to the other chromite layers for Ni, Cu,

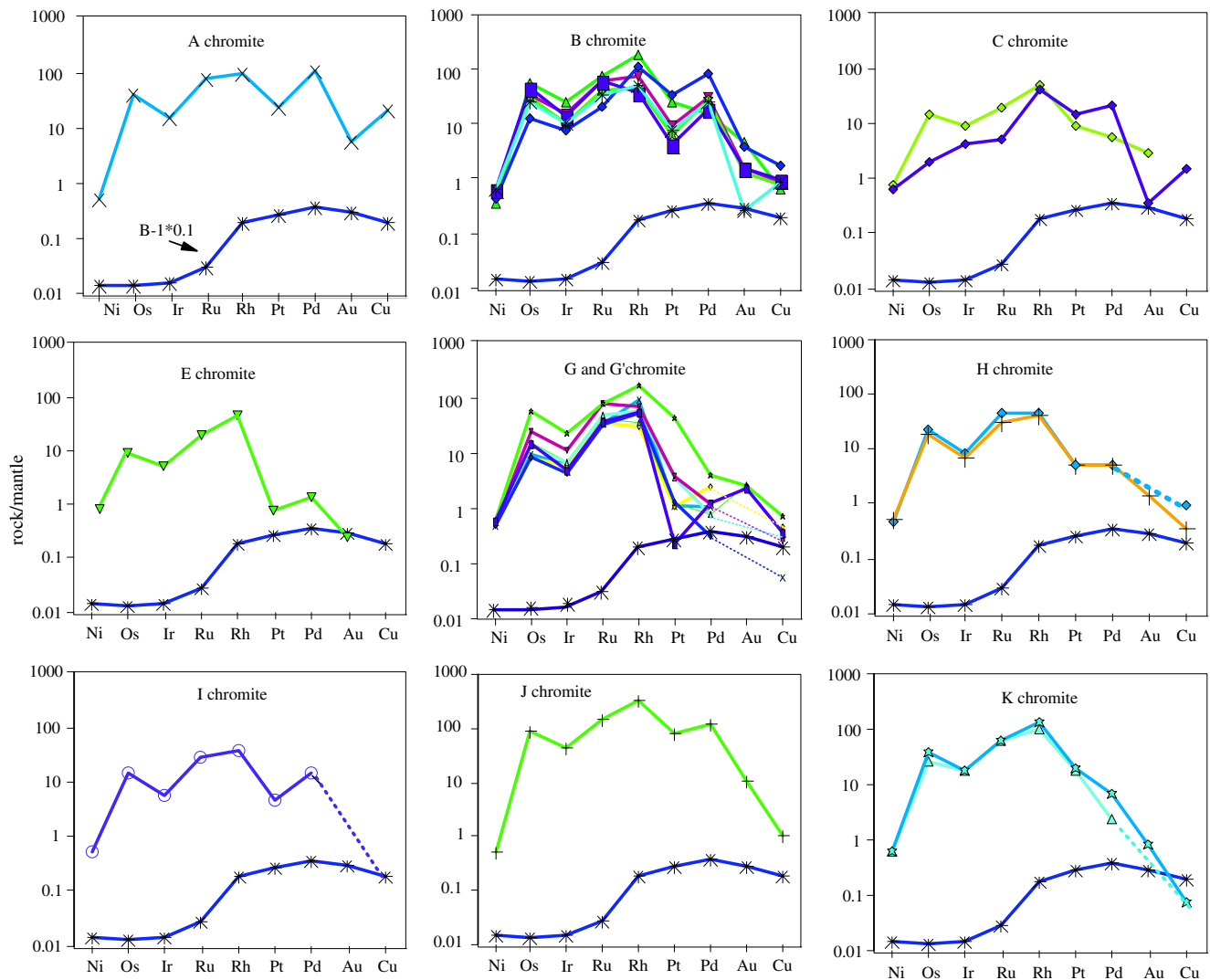


Fig. 9 Whole rock mantle normalized patterns for the chromite layers of the Stillwater Complex: *Asterisk*=pattern for 10 % trapped liquid fraction

IPGE, and Rh; they are strongly depleted in Pt, Pd, and Au relative to IPGE and Rh (Fig. 9).

Assuming 10 to 20 % trapped liquid fraction, all the chromite layers show enrichment in IPGE and Rh of three orders of magnitude (Figs. 2 and 9). For most chromite layers, Pt and Pd show some enrichment of one to two orders of magnitude (Figs. 2 and 9). The G chromite layers show much less enrichment. Much of the Cu and Au concentrations in all of the chromite layers and much of the Pt and Pd in the G chromite layer could be accounted for by trapped liquid fraction (Fig. 9).

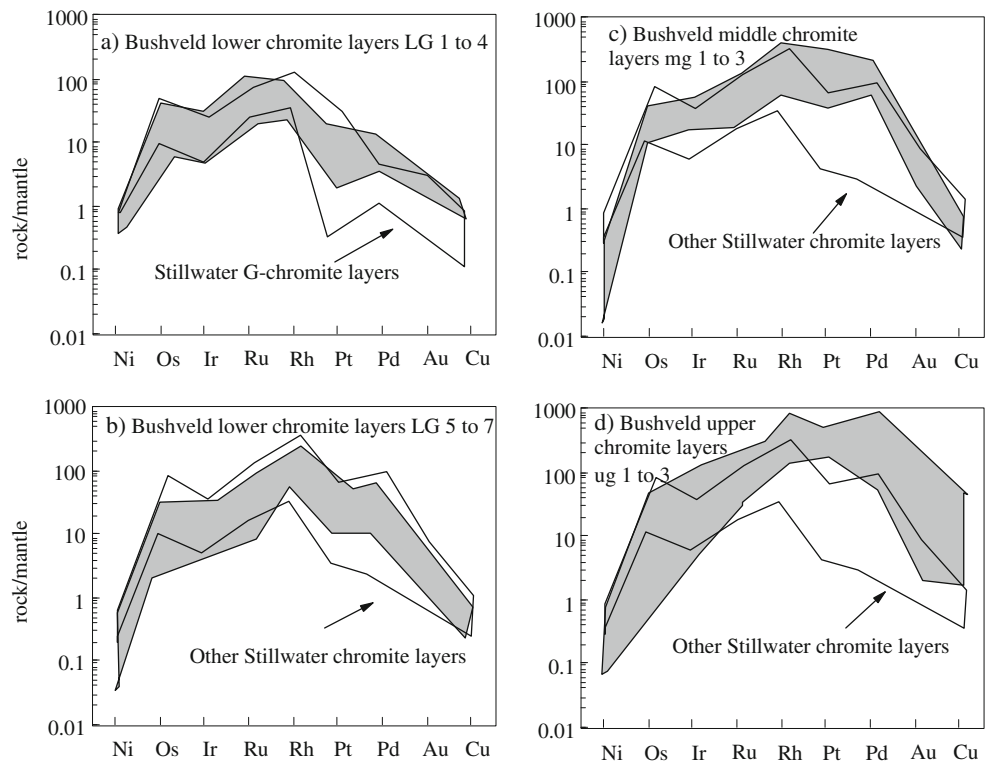
Chromite layers from the Bushveld Complex and Great Dyke show an evolution in the PGE patterns with stratigraphy. The lower most layers from the Bushveld complex, the LG1 to 4, show flat mantle-normalized patterns from Os to Rh and then decrease from Pt to Cu (Fig. 10a). The overlying layers show a progressive increase in Rh, Pt, and Pd through the LG5 to 7 (Fig. 10b) and the MG1 to 3 (Fig. 10c) to the UG1 to 3 (Fig. 10d). As a result, the peak in the PGE patterns is at Rh in

the LG5 to 7 layers and at Pt and Pd in UG1 to 3 layers. The lower chromite layers from the Great Dyke also show a strong enrichment in IPGE (Fig. 11a), the middle chromite layers have positive Rh anomalies (Fig. 11b), and the upper chromite layers show an increase in Pt and Pd (Fig. 11c).

Unlike the Bushveld and Great Dyke complexes, the lower chromite layers at Stillwater are not the most depleted in Pt and Pd. The $(Pd+Pt)/(Os+Ir+Ru+Rh)$ ratios decrease from the A to G chromite layers and then increase again through the H to K layers (Fig. 2). The G layers most closely resemble the lowermost chromite layers of the Bushveld (LG1 to LG4) and Great Dyke complexes (Figs. 10 and 11a). The Bushveld and G chromite layers show the closest similarity, whereas some of the Great Dyke chromite layers are richer in Ir and Ru and most are poorer in Rh.

The other chromite layers from Stillwater appear to most closely resemble the LG5 to 7 layers of the Bushveld complex, both in level and shape (Fig. 10b) and are depleted in Pt,

Fig. 10 Whole rock mantle-normalized metal patterns for chromite layers of the Bushveld Complex compared to the Stillwater Complex chromite layers. The Stillwater chromite layers most closely resemble the lower group chromite layers of the Bushveld. Data for the Bushveld chromite layers from Barnes and Maier (2002) and references therein and Naldrett et al. (2009)



Pd, and Au relative to the middle group chromite and the upper group chromite layers of the Bushveld complex (Fig. 10c, d). Compared to the Great Dyke chromite layers, the Stillwater layers most closely resemble the upper chromite layers (c1d) although some Great Dyke samples are enriched in Pd relative to the Stillwater chromite layers (Fig. 11c).

Discussion

Which minerals host the platinum-group elements?

Most of the rocks from the Ultramafic series are enriched in PGE relative to the trapped liquid component, and in particular, they are enriched in IPGE and Rh (Figs. 2, 8, and 9). Thus, some phase(s) have collected all of the PGE, and in addition, IPGE and Rh have been preferentially enriched.

Various lines of evidence suggest that chromite could be the phase collecting the IPGE and Rh. The chromite layers are richer in IPGE and Rh than the silicate layers (Figs 2, 8, and 9, Table E6); and experimental work (Righter et al. 2004; Brenan et al. 2012) has shown that these elements can partition into chromite. Furthermore, chromite phenocrysts from volcanic

rocks have been shown to be enriched in IPGE and Rh (Locmelis et al. 2011; Pagé et al. 2012; Pagé and Barnes 2013; Park et al. 2012). Plots of Cr₂O₃ versus the IPGE and Rh at Stillwater show a strong positive correlation between IPGE, Rh, and Cr₂O₃ (Fig. 12). In spite of this in situ analysis of chromite grains found that the concentrations of IPGE and Rh in the chromite are less than the detection levels and that chromite accounts for less than 15 % of the IPGE and Rh budget in the Stillwater chromite layers (Pagé et al. 2012). Thus, although IPGE, Rh appears to have accumulated in the chromite-bearing rocks; these elements are not in the chromite.

The phase controlling the IPGE could be laurite. Inclusions of laurite are commonly observed in chromites from layered intrusions and ophiolites (González-Jiménez et al. 2013; Maier et al. 1999; Prichard et al. 2008), and as described above, Stillwater chromites are no exception. The Stillwater laurite contains IPGE and, in some cases, Rh (ESM 4). If we consider the G chromite layers (because most samples contain <10 ppb Pd, ESM 6, and thus probably do not contain a cumulate sulfide component), then we can estimate the number of laurite grains required to accommodate the Ru present in the rock by:

$$\frac{(\text{concentration of Ru in rock})}{[(\text{area PGM grain}/\text{area polished section}) \times (\text{density laurite}/\text{density chromite}) \times (\text{wt \% Ru in laurite}/100)]}$$

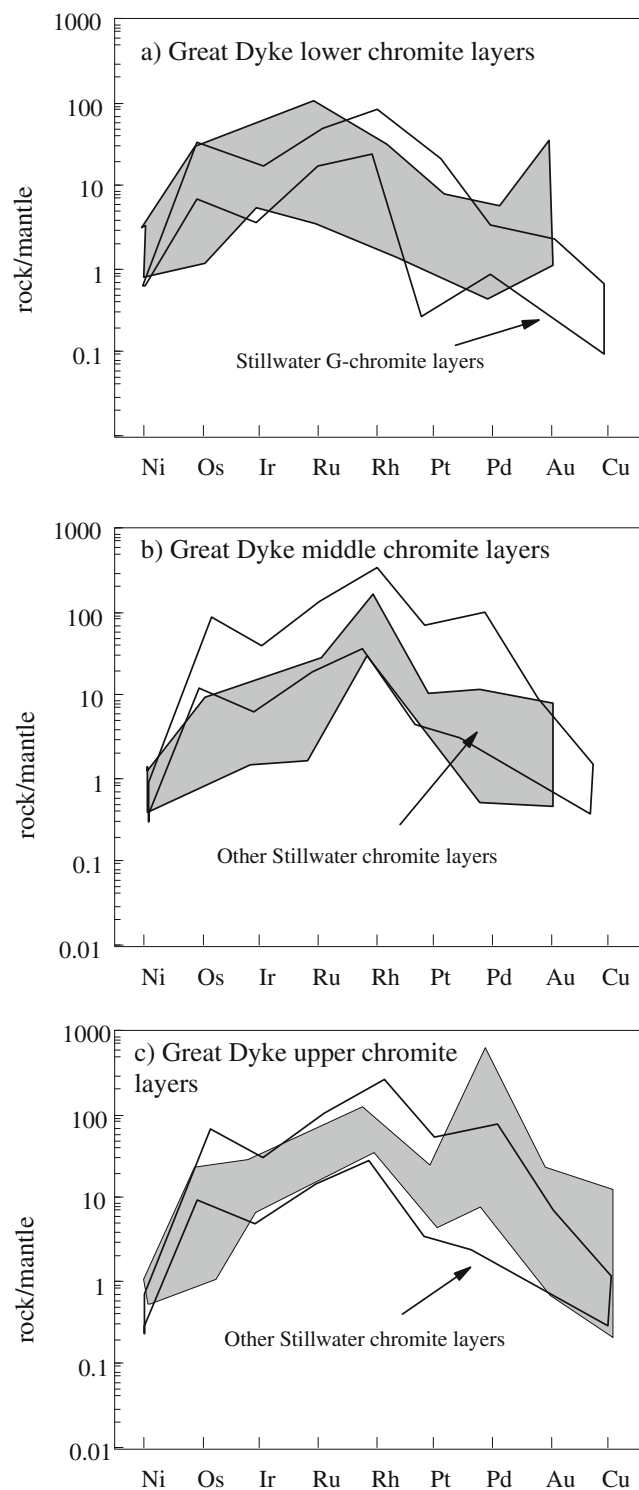


Fig. 11 Whole rock mantle normalized patterns of the chromite layers from the Great Dyke compared with the chromite layers of the Stillwater Complex. Data from Oberthür (2002)

Assuming that the diameter of a laurite grain is $\sim 5 \mu\text{m}$ (based on the SEM observations, ESM 4), this is equivalent to ~ 7 grains of laurite per thin section similar to the number of grains observed (31 grains were observed in 7 thin sections of

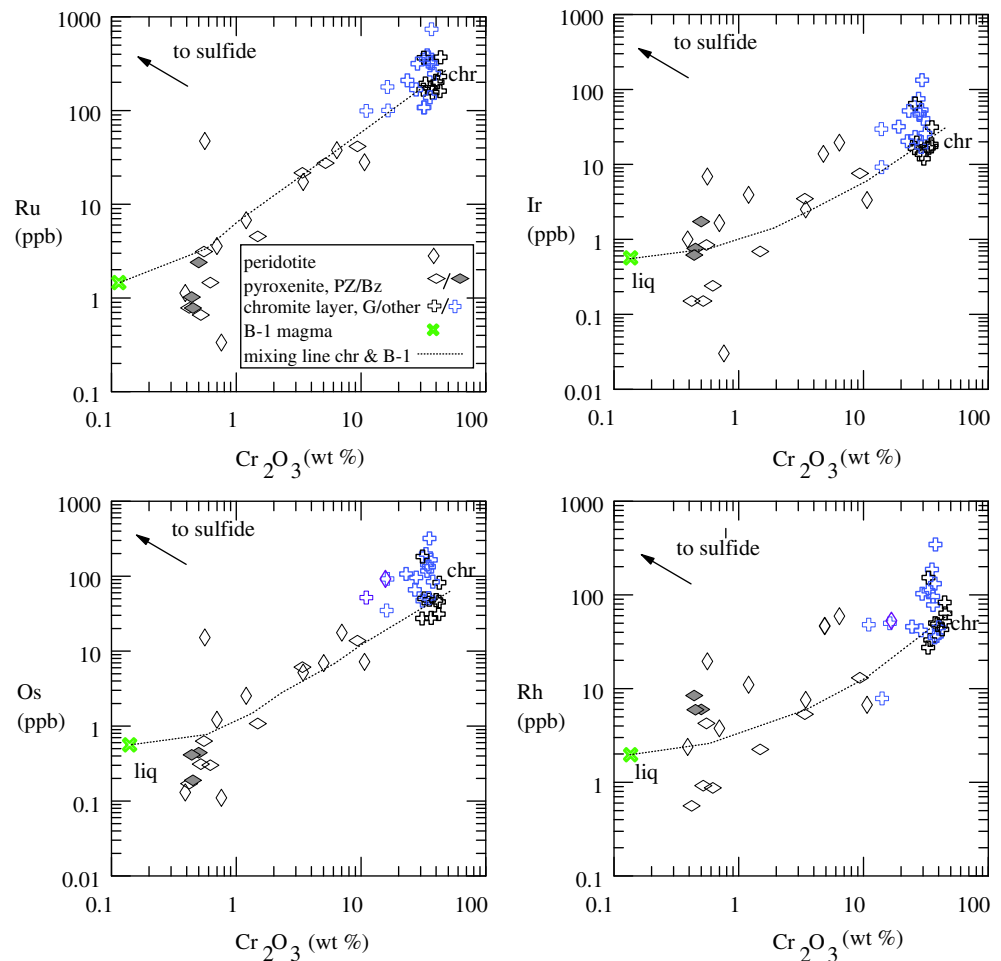
the G-chromite, ESM 4), which suggests that laurite is indeed the major host of Ru. It should be mentioned that this method of estimation is a rough approximation because a thin section only samples a small volume of material. For example, based on the tables from Potts (1987) for a grain size of $5 \mu\text{m}$ and 200 ppb Ru, one would need to examine five polished section before a 1 sigma error on the estimation would be less than 20 relative percent. If the grain size was $10 \mu\text{m}$, then 20 polished sections would be required to achieve the same precision. In other words, if the PGM grain size is large and the concentration of the element low, then the thin section will not necessarily contain a representative number of grains (Godel 2013). Nonetheless, considering the ubiquitous presence of laurite in the chromite layers (in total 143 grains of laurite were observed in the 29 polished sections that were examined), we consider that the conclusion that laurite is the major host of Ru is justified.

If laurite is also the major host for Os, Ir, and Rh, then the ratios of Ru/Os, Ru/Ir, and Ru/Rh of the whole rock should be similar to that of the laurites. The Ru/Ir ratio of the laurites and the G chromite layers are similar, in the 8 to 16 range, and thus laurite could be the major host for Ir in these layers (Fig. 13a). However, in the other layers, the Ru/Ir ratio is lower than that of the laurites, and thus, in addition to being present in laurite, Ir must be present in another phase. The Ru/Os and Ru/Rh ratios of the whole rocks are distinctly lower than those of the laurites (Fig. 13a, b), especially in the case of Rh where the ratio of the laurites is four times that of the whole rock. This suggests that another phase is required to accommodate some of the Os and much of the Rh.

The inclusions contain a few grains of Rh-bearing sulfide. Two grains of ~ 5 microns in diameter were large enough to analyze and appear to be Rh-rich malanite (CuPt_2S_4) (ESM 5). Some of the samples plot close to tie lines between laurite and malanite on a triangular plot of Pt–Rh–Ir (Fig. 13c). However, malanite and laurite alone are insufficient to account for the Rh enrichment found in samples because many of the G chromite layers and the E pyroxenites plot above the laurite–malanite tie line towards the Rh pole. Furthermore, the number of malanite grains observed (a total of 5 in 31 polished sections, ESM 5) is insufficient to account for the Rh. If the Rh had been largely hosted in malanite grains, ~ 64 grains should have been observed. Base metal sulfides in layered intrusions have been shown to contain most of the PGE (with the exception of Pt). Small amounts of pentlandite and millerite are present in the Stillwater samples, and these minerals have been shown to accommodate both Rh and Pd in other mafic intrusions, supporting the idea that sulfides could be the carrier for some of the PGE. Preliminary analyses of the sulfide grains from layers B, G, and J (these layers contain grains large enough for analysis by laser ablation) show that, on average, they contain PGE in 20 to 400 ppm range (ESM 3).

A mass balance has been carried out (ESM 3, Fig. 14) for the average whole rock concentrations of the chromite layers.

Fig. 12 Plots of IPGE and Rh versus Cr₂O₃ showing strong positive correlations between the PGE and Cr₂O₃. Dashed line mixing line between chromite from Bushveld chills and B-1 liquid



To do this, we used the average composition of the base metal sulfides and assumed that the amount of laurite present in the average chromite sample is similar to that in G layer. We believe this assumption to be justified because the number and size of laurite grains is similar in most layers. It should be stressed that this calculation is only an approximation. Nonetheless, it gives an idea of which minerals are controlling each element. The mass balance shows that most of the Ru, Ir, and Os are present in laurite, with approximately 10 % in base metal sulfides. In contrast, Rh is largely present in the sulfides with only 12 % in laurite. The majority of the Pd is present in the sulfide.

As has been found in previous studies of magmatic sulfides (Djon and Barnes 2012; Godel and Barnes 2008; Smith et al. 2014), very little of the Pt is accommodated in the base metal sulfides. As mentioned above, small (<2 μm) grains of Pt minerals are present both in the inclusions (Fig. 5b) and in association with the interstitial base metal sulfides. We conclude that Pt is hosted by these minerals.

To summarize, the chromite layers are generally enriched in all of the PGE, in particular in IPGE and Rh. Ruthenium, Os, and Ir are accommodated largely by laurite, with minor

amounts in base metal sulfide. Rhodium is accommodated in base metal sulfide with minor amounts present in laurite. Palladium is present mainly in base metal sulfides. The hosts of Pt are the Pt minerals present associated with the base metal sulfides.

Most of the pyroxenites and peridotites have mantle-normalized metal patterns which are not as enriched in PGE as the chromite layers, but nonetheless show similar characteristics with enrichment in IPGE and Rh, which suggests that they too contain a small amount of laurite and base metal sulfide.

Models for the enrichment of PGE in chromite layers

Any model for the origin of the distribution of PGE in the Ultramafic series of Stillwater must explain: (a) why the chromite layers are enriched in IPGE and Rh, (b) why some layers are enriched in Pd and Pt and some are not, and (c) how the IPGE became to be largely present in laurite, Pd, and Rh in base metal sulfides and Pt (in Pt minerals). Also, given the similarity in the composition of the Bushveld and Great Dyke

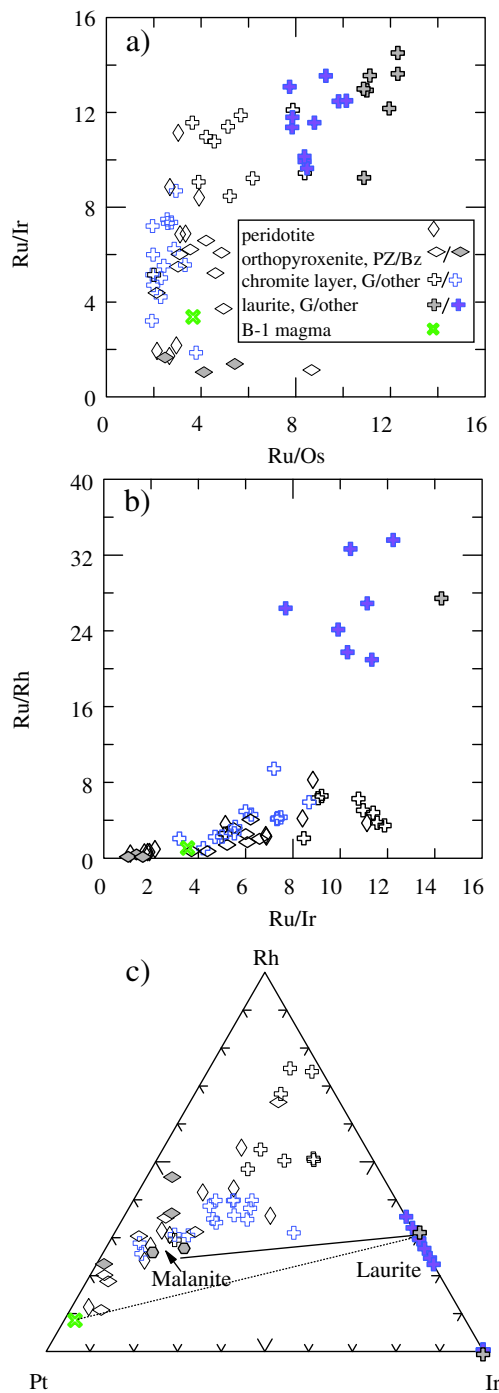


Fig. 13 Comparison of whole rock and platinum-group mineral compositions: **a** Ru/Ir versus Ru/Os, **b** Ru/Rh vs Ru/Ir; both of these plots show that the rocks have lower Ru/Ir Ru/Os and Ru/Rh ratios than the laurites, indicating an additional phase is needed to accommodate the Os, Ir, and Rh. **c** Triangular plot of Pt, Rh, and Ir showing the sample plot above the laurite–malanite and laurite–magma tie lines, indicating that a Rh-rich phase is necessary to account for the distribution of the samples

chromite layers, the model should also be applicable to these intrusions. Three models to do this are considered.

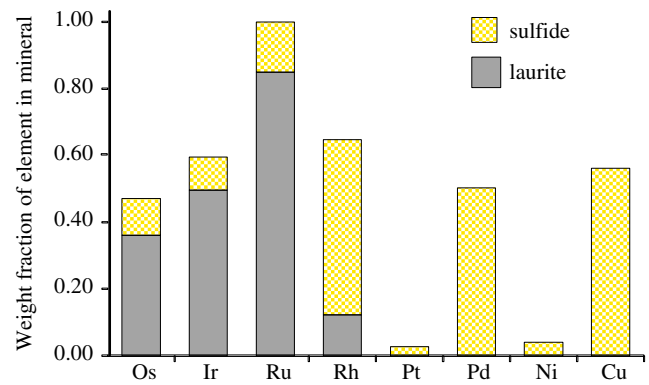


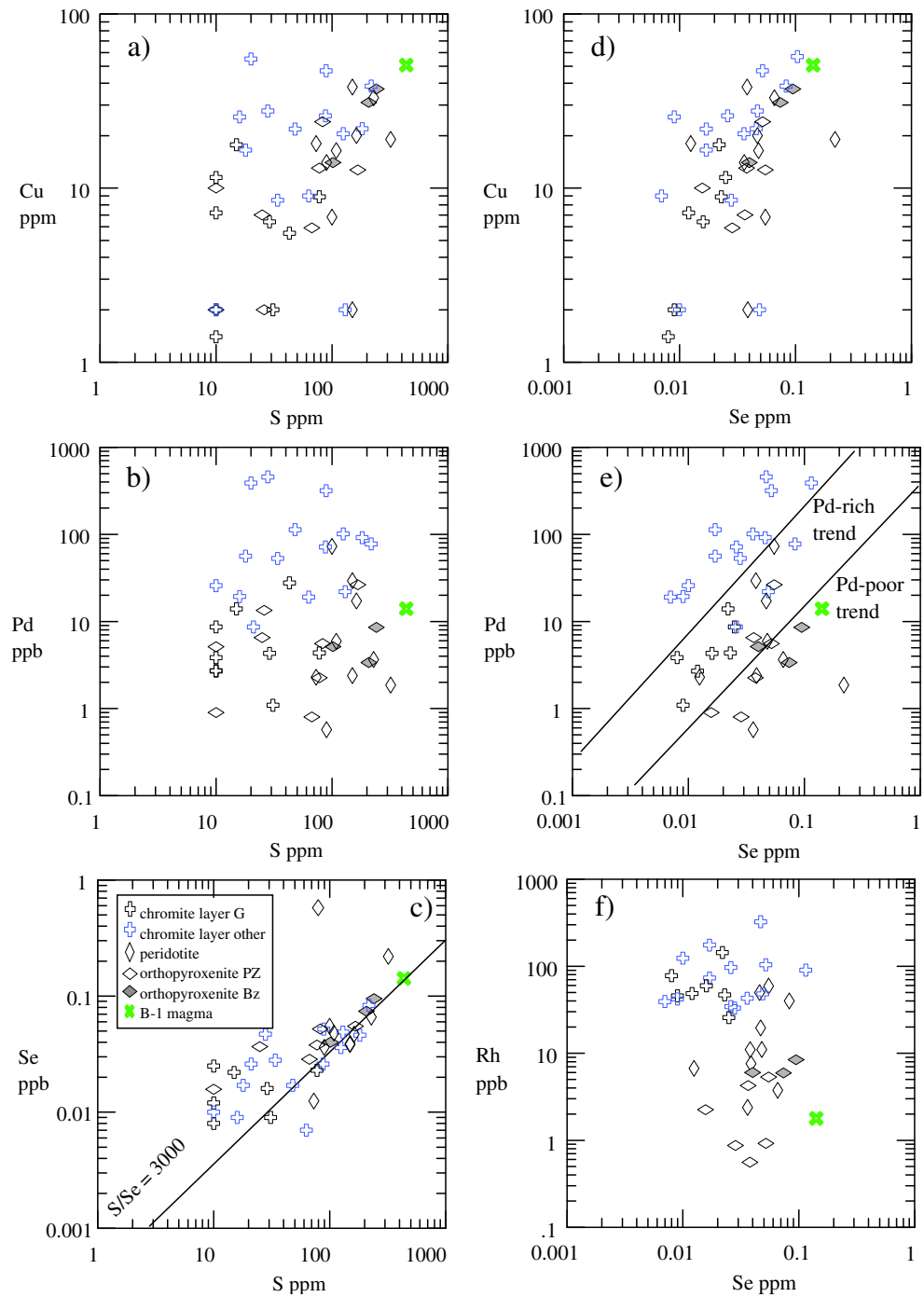
Fig. 14 Mass balance for the PGE, Cu, and Ni for the average chromite layer showing that Os, Ir, and Ru are largely controlled by laurite with a minor contribution from base metal sulfides. Rhodium is controlled by both laurite and base metal sulfides. Palladium and Cu are controlled mainly by sulfides. The phase controlling Pt has not been identified

Collection of PGE by a base metal sulfide liquid followed by S, Pd, and Pt loss

Given the high partition coefficients of the PGE between sulfide and silicate liquids (Peach et al. 1990; Crocket and Fleet 1997; Mungall and Brenan 2014), it is reasonable to consider the possibility that the PGE was collected by a base metal sulfide liquid. However, the rocks contain too little S for cumulate sulfides to be present, and the PGE and Cu do not show positive correlations with S (Cu and Pd illustrated in Fig. 15a, b, correlation matrix in ESM 7). One possible explanation for this is that more sulfides were originally present in the rocks, but subsequently, S has been removed from the rocks. As mentioned in the mineralogy section, the sulfide grains are partly altered to magnetite and (or) the assemblage of sulfides contains minerals such as bornite and millerite, which suggests the sulfide assemblage has been altered from a primary igneous assemblage. Similar observations have been made in the Bushveld rocks (Kanitpanyacharoen and Boudreau 2013; Li et al. 2004). The hypothesis of S loss may be considered by investigating the S/Se ratios. Primary magmas generally have S/Se ratios close to mantle values (~3000, McDonough and Sun 1995). Selenium is considered to be less mobile than S; thus, S loss leads to low S/Se values. On a plot of Se versus S (Fig. 15c), rocks with >100 ppm S have S/Se ratios close to mantle and rocks with <100 ppm S have values much less than mantle and plot on the S depleted side. Based on the low S/Se ratios, many of the samples from the chromite layers have experienced substantial S loss.

Assuming that Se is immobile, it can be used as a proxy for S to determine whether a sulfide liquid collected the chalcophile elements. A plot of Cu versus Se shows a positive correlation and consistent with collection by a sulfide liquid (Fig. 15d). A plot of Pd versus Se (Fig. 15e) shows two trends. One defined by the chromite layers which have high Pd/Se

Fig. 15 Bivariate plots of Cu, Pd, S, Se, and Rh to investigate the possibility of control of the elements by a sulfide liquid. **a, b,** and **c**, Cu, Pd, and Se versus S showing that in rocks containing <100 ppm S, the metals do not show a correlation with S. **d** and **e** Show that Cu and Pd correlate with Se. **f** Shows Rh does not correlate with Se



ratios (~3) and a second trend with lower Pd/Se (0.3) ratios defined mainly by the pyroxenites. These trends could represent mixing of sulfide liquid with a cumulate of silicate minerals and chromite (both of which would have contained very little of either element). The presence of two trends may reflect the presence of sulfide liquids with different Pd contents. The reason for the sulfide liquids having different Pd contents is that the partition coefficient of Pd into sulfide liquid is very high and much higher than that of Se (Patten et al. 2013; Peach et al. 1990). Consequently, Pd is much more readily

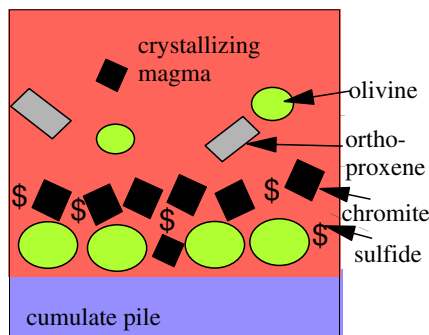
influenced by the segregation of a sulfide liquid than Se, and thus, sulfides that form first are much richer in Pd than the sulfides that segregate from the more fractionated liquid. The concentration of Se in the silicate liquid does not change a great deal. Therefore, the Pd/Se ratio decreases as the magma fractionates. If these trends do indeed represent control by a sulfide liquid, then after crystallization, much of the S in the chromite layers were removed.

Whereas collection by sulfide liquid followed by S loss may account for the distribution of Cu and Pd, it is

insufficient to account for the distribution of the other PGE. If a sulfide liquid alone controlled the PGE, then the shape of the metal patterns would resemble that of the silicate liquid from which it segregated because all the partition coefficients of all the PGE between sulfide and silicate liquid are very high (Barnes et al. 1988). In addition, if sulfide liquid was the only phase controlling the collection of the PGE, they should show a positive correlation with Se, which the IPGE and Rh do not (Rh vs Se illustrated in Fig. 15f).

Many of the studies on Stillwater favor a model where fluids have a role in collecting the PGE (Boudreau et al. 1986; Hanley et al. 2008; Aird and Boudreau 2013). Building on their suggestions, one could postulate that all of the PGE initially were collected by a base metal sulfide liquid and deposited on the cumulate pile (Fig. 16a). The sulfide liquid concentrated with the chromite due to their high densities relative to the silicates. Subsequently, the magma became saturated in hydromagmatic fluid which partly dissolved the

a) Collection of chromite and base metal sulfide on a the cumulate pile



b) Saturation of magma in fluid
Partial dissolution of sulfides and mobilization of Pd, Se, +/-Pt.
Exsolution of RuS₂, PGM
formation of bornite and millerite

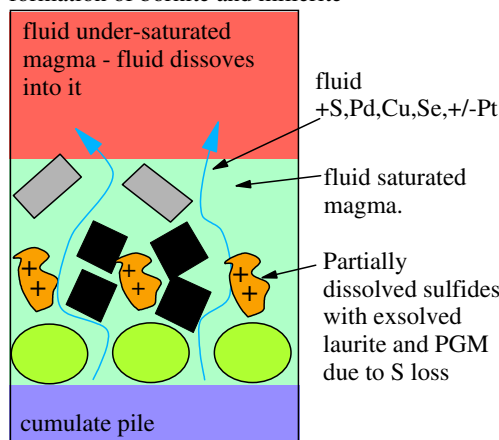


Fig. 16 Model of collection of PGE by base metal sulfides followed by S, Pd, Cu and Se loss

sulfides and partly removed Cu, Pd, and, to a lesser extent, Pt (Fig. 16b) leaving the rocks showing variable depletion in these elements. Aird and Boudreau (2013) examined the sulfides in three samples from the Ultramafic series and report that they are associated with carbonates which led them to propose that the fluid was carbonate rich. The fluid rose through the cumulate pile and dissolved into the overlying fluid-undersaturated magma enriching this magma in Pd relative to all the other PGE.

The partial removal of Pd from the cumulate could also explain the observation that the Pt/Pd ratios of the rocks of the Ultramafic series vary considerably from 1 to 10 (Fig. 17). Using the fluid model, it could be argued that variable proportions of Pd have been removed from the rocks by the hydromagmatic fluid. The mobility of Pd is of particular interest because the JM reef is Pd-rich with Pd/Pt ratio of approximately 3 (Zientek et al. 2002), whereas both the reefs of the Bushveld and Great Dyke generally have Pd/Pt ratios in the 0.5 to 1.5 range (Barnes and Maier 2002; Oberthür 2002). The high Pd/Pt ratios in the JM reef could be due to the magma becoming progressively enriched in Pd which was contributed from the hydromagmatic fluid.

The presence of laurite inclusions in chromite and the concentration of Rh and Pd in base metal sulfide can be explained as follows. Experimental work demonstrates that the loss of S from magmatic sulfides leads to the exsolution of PGM from the sulfides (Ballhaus et al. 1994; Peregoedova et al. 2006). As the base metal sulfides in the chromite layer were dissolved by the fluid, laurite and Pt minerals exsolved from the sulfides. Rhodium and any Pd are not dissolved by the fluid concentrated into remaining sulfide. The inclusion of the PGM and some base metal sulfides within chromite grains could be the result of their inclusion during sintering of the chromite grains during cooling. Essentially, the residual base metal sulfides and associated PGM are caught at triple junctions formed between

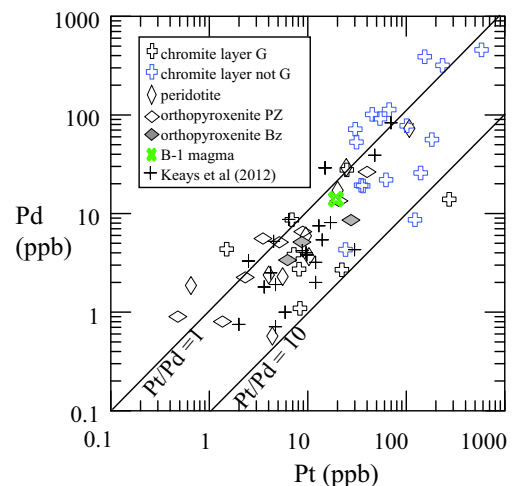


Fig. 17 Pt versus Pd showing that most of the samples have Pd/Pt ratios less than 1

chromite grains during post-cumulate growth (Fig. 3e). As the small chromite grains combine to form larger grains, the sulfide and PGM were included in the new large grains.

The changes in the mantle PGE-normalized patterns of the Great Dyke and the Bushveld chromite layers suggest that there is some stratigraphic control on the processes that concentrated the PGE in these two intrusions. For the Great Dyke chromite layers, the peak in the mantle-normalized patterns is at Ru in the lower chromite layers and at Rh in the higher layers (Fig. 11). Palladium enrichment is only evident in the uppermost layer. In the case of the Bushveld chromite layers, the lowermost layers (LG1 to 4) are enriched in both Ru and Rh. The enrichment shifts to Rh in the LG5 to 7 (Fig. 10). The amount of Pt and Pd increases up in section, and in the middle and upper group chromite layers, Rh, Pt, and Pd are present in sub-equal amounts, resulting in flat mantle-normalized patterns (Fig. 10). The fluid model has been considered for the Bushveld (Kanitpanyacharoen and Boudreau 2013) and may also apply to the Great Dyke chromite layers. One difference between the Stillwater Ultramafic series and the ultramafic rocks of both these intrusions is that there appears to be an evolution in the PGE patterns with increasing stratigraphic height. The lower chromite layers are depleted in Pt, Pd, and Cu relative to the IPGE and Rh, and the upper layers show increasing amounts of Pt, Pd, and Cu (Figs. 10 and 11). The fluid model would require that the amount of Pt, Pd, and Cu dissolved by the fluid was at the maximum in the lower layers and decreased up section. Whereas at the Stillwater rocks, the maximum dissolution was in the middle of the Ultramafic series in the G layers.

One difficulty with this model is that it requires a relatively high solubility of Pd and Pt in high temperature magmatic fluids. Tagirov et al. (2013) reported that at 600 °C and at geologically reasonable pHs, near-neutral solutions can transport up to several ppm of Pd. However, mobility of Pd in higher temperature fluids at reasonable pHs has yet to be demonstrated (Bazarkina et al. 2014).

Another problem is that the IPGE and Rh do not show a positive correlation with Se. If these elements were initially collected by a base metal sulfide liquid and if Se is immobile, then one should expect to see a correlation. Finally, Pd and Cu do show positive correlations with Se (Fig. 13d, e). Thus, this model requires that Pd, Cu, and Se were mobilized to a similar degree.

Collection of the PGE by PGM and sulfide liquid followed by S loss

The enrichment of chromite-rich rocks in IPGE has noted in many environments, and the Bushveld chromite layers have received particular attention Merkle (1992). Recently, Naldrett et al. (2009) reported that in these chromite layers, Os, Ir, Ru, and Rh show positive correlations with each other, but not

with Pt and Pd. The classic model for enrichment of PGE in chromite layers is that PGM, in particular laurite, crystallize in the presence of chromite (Hiemstra 1979; Kinloch 1982; Brenan and Andrews 2001). These small crystals are included in chromite and collect on the cumulate pile together with chromite. Laurite is observed both in the Stillwater and Bushveld chromite layers; thus, collection of IPGE by laurite is considered a reasonable model. The behavior of Rh and Pt is not generally closely considered, but implicit in this model is that these elements also crystallize early as PGM.

Experimental work on simple basalt analogues consisting of SiO₂, Al₂O₃, MgO, and CaO (CMAS) has shown that the solubilities of the PGE are critically dependent on the fugacity of oxygen and temperature. At oxygen fugacities close to the fayalite–magnetite–quartz (FMQ) buffer and the temperature of crystallization of chromite (1200–1300 °C), the solubilities of Ir, Ru, and Pt are in the 1–20 ppb range (Blaine et al. 2005; Borisov 2005). These concentrations are similar to the concentrations of PGE in mafic magmas, and thus, it seems plausible that the melt could have crystallized PGM rich in IPGE and Pt. However, recent experiments by Laurenz et al. (2013) included FeO and S in the experiments and found that the Ru solubility was four times greater in the presence of FeO and orders of magnitude greater in the presence of S than in the CMAS basalt, which would mean the magma would not attain laurite saturation under equilibrium conditions. Finnigan et al. (2008) carried out experiments that may provide a solution to this and explain why the PGM is found in chromite. They showed that IPGM could crystallize in the boundary layer of chromite grains because this boundary layer is slightly reduced due to the preferential removal of Fe⁺³ from the silicate liquid by chromite.

As mentioned above at Stillwater, the samples have variable Pt/Pd ratios in the range 1 to 10 (Fig. 17). In the samples with high Pt/Pd ratios, it could be argued that Pt-rich mineral has crystallized. Furthermore, chromite phenocrysts from volcanic rocks has been shown to contain small Pt–Fe inclusions (Park et al. 2012) which may be the product of Pt–Fe alloys crystallization. In this model, Pt minerals crystallized in the boundary layer of some of the chromite and are included in the chromite. However, at Stillwater, although most of the chromite layers are enriched in Pt, unlike the IPGE and Rh, Pt does not show a strong correlation with Cr₂O₃; therefore, crystallization of a Pt-rich mineral in the chromite boundary layer is not the only process controlling Pt. Possibly, there are two processes which influenced Pt, namely in rocks formed when the magma was undersaturated in base metal sulfide liquid, a small amount of Pt crystallized as a Fe–Pt alloy, but when the magma was saturated in sulfide liquid, Pt was controlled by the sulfide liquid. Thus, in magma undersaturated in sulfide liquid, Pt was collected by Fe–Pt alloy and this enriched the cumulate in Pt over Pd. However, once sulfide saturation occurs both Pt and Pd partitioned into the sulfide liquid,

collected on the cumulate pile and the cumulates have Pt/Pd ratio similar to the magma. In this model, the erratic crystallization of a Pt alloy in the chromite boundary layer is the reason that many, but not all, of the Ultramafic series samples have Pt/Pd ratios greater than one (Fig. 17).

Collection of IPGE by laurite and Pt by a Pt alloy cannot account for the all the PGE found in the Stillwater rocks. As can be seen in Figs. 8, 9, and 18, most of the rocks contain more Pd and Rh than can be accommodated by the trapped silicate liquid fraction and laurite. The Bushveld and Great Dyke rocks also contain too much Rh and Pd to be accommodated by laurite (Figs. 10, 11, and 18). The solubility of Pd and Rh in a basaltic magma is high, in the 1–10 ppm range (Borisov 2005; Ertel et al. 1999; Laurenz et al. 2013); thus, the excess Pd and Rh in the rocks cannot be due to crystallization of Pd or Rh minerals. The host of these elements now is pentlandite which leads to the conclusion that they were collected by sulfide liquid. The magma would only have become saturated with the sulfide liquid after the crystallization of laurite and other PGM because laurite does not crystallize in the presence of sulfide liquid in natural systems (Brenan and Andrews 2001). The reason for which laurite does not crystallize in the presence of sulfide liquid is because the concentrations of Ru are required to bring about laurite saturation in both the sulfide liquid and silicate liquid at the same time are much higher than found in natural rocks.

When a magma becomes saturated in a sulfide liquid, the sulfide occurs as small (1–10 μm) dispersed droplets such as those observed in MORB basalts (Patten et al. 2012). In order for the Pd to be introduced into a chromite layer, the sulfide liquid would have to have percolated through the partially consolidated cumulate pile to the chromite layer. Provided that the sulfide droplets were smaller than narrowest interconnected interstitial pore space, the sulfide droplets could migrate downwards while displacing silicate liquid (Chung and Mungall 2009). The grain size of the cumulate silicates (1–10 mm) is such that the diameter of the interstitial pore space prior to compaction of the cumulate pile would have been much larger than that of the migrating sulfide droplets (assuming the current size of the sulfides, <0.01 to 0.1 mm, represents the size of the sulfide droplets). In contrast, the size of the chromite grains (0.1 mm) is such that the interstitial space between chromite grains was small, and thus, the sulfide droplets could have migrated through the silicate part of the cumulate until they were trapped in the small pore spaces in chromite layers, thereby enriching the chromite layers in PGE.

The idea that most chromite layers from the Bushveld, Stillwater, and Great Dyke complexes contain a sulfide liquid component is difficult to reconcile with the very low S content of the chromite layers, <300 ppm (Naldrett et al. 2009; this work, Oberthür 2002). Naldrett and Lehmann (1988) suggested a model to account for this, and Naldrett et al. (2009) expand on this in more detail. They argue that during cooling,

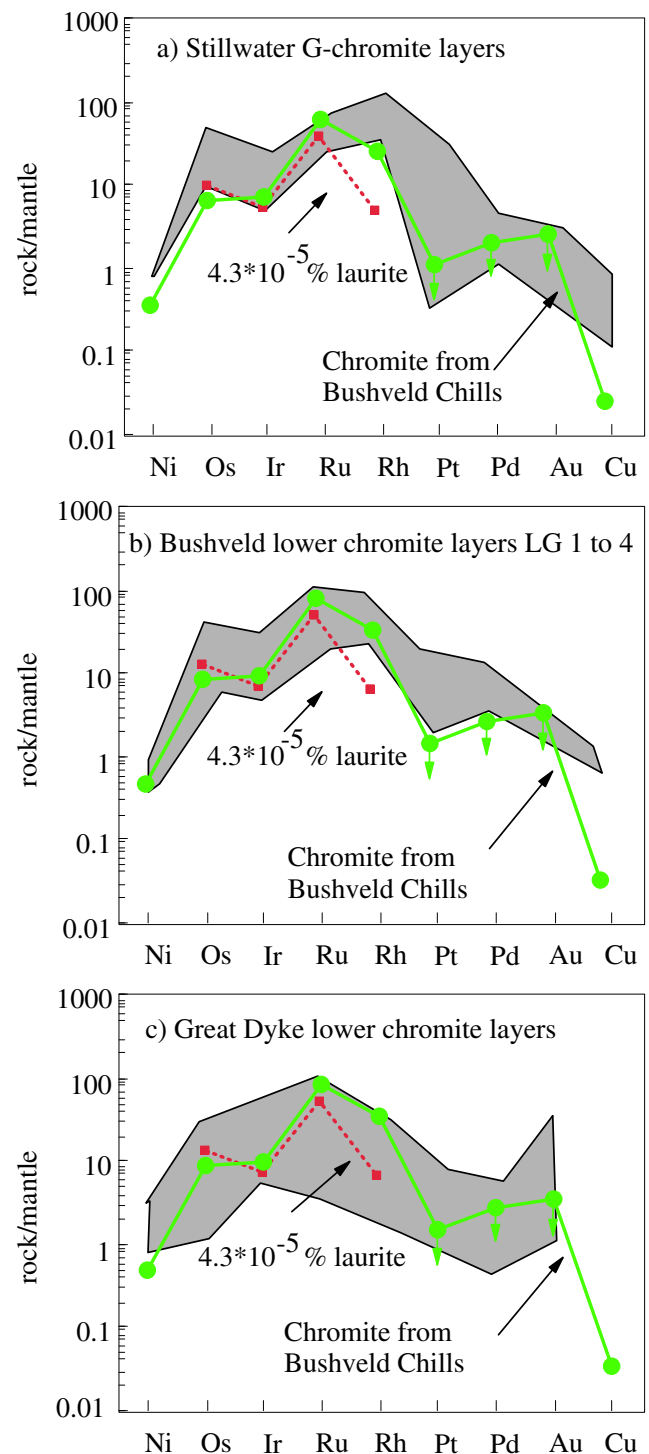


Fig. 18 Comparison of mantle-normalized metal patterns of the G-chromite layers, the LG1–4 chromite layers, and the Great Dyke lower chromite layers with patterns of chromite from Bushveld chill (Pagé and Barnes 2013) and with laurite. Note that the shape of the metal pattern of the Bushveld chill chromite shows stronger similarities with chromite layer patterns than the laurite does. Downward arrows indicate values less than detection limit

Fe from the sulfides diffused into the chromite to fill vacancies in the chromite. The loss of Fe from the sulfide led to a release

of S, and hence, the amount of sulfides now observed in the chromite layers does not reflect the original amount of S present. We presented evidence above that at Stillwater, the sulfide mineralogy and the low S/Se ratios of many of the chromite layers support the idea that S has been lost from the Stillwater chromite layers; this could be the result of Fe loss to the chromite followed by S loss from the sulfide.

This model has problem in modelling the Rh contents of the chromite layers. Rhodium correlates with the IPGE and Cr_2O_3 , suggesting the same process collected Rh, IPGE, and Cr_2O_3 . Some of the laurite contain a little Rh (ESM 5), but the laurites have a much higher Ru/Rh ratio than the whole rock (Fig. 13b), i.e., the laurites do not contain enough Rh to accommodate all the Rh in the chromite layers. Collection by another PGM Rh-rich PGM is not a viable solution because Rh is fairly soluble in basalt (Ertel et al. 1999; Fortenfant et al. 2003). Finally, our observations suggest that Rh is now mainly hosted by base metal sulfide rather than a PGM.

Collection of IPGE and Rh by chromite, followed by base metal sulfide addition and S loss

Despite the strong correlations between the IPGE, Rh, and Cr_2O_3 (Fig. 12, ESM 7), the hypothesis that IPGE and Rh partitioned into chromite and chromite acted as a collector does not appear to be viable because these elements are not now present in chromite, but rather are found in laurite and base metal sulfide. However, the idea deserves re-examination in light of: the significant correlation between Rh and Cr_2O_3 , the lack of correlation of Rh with Se, and the recent observation that chromites phenocrysts from volcanic rocks and chromites from the sills in the Bushveld margins are enriched in IPGE AND Rh (Pagé et al. 2012; Pagé and Barnes 2013; Park et al. 2012). Empirical partition coefficients calculated from most of these phenocrysts are generally similar for Os, Ir, and Rh and in the 10 to 100 range (Pagé et al. 2012; Pagé and Barnes 2013). The partition coefficients for Ru are slightly higher in the 50 to 140 range. The chromite phenocrysts from oxidized magmas from arc settings give high partition coefficients in the 200 to 1000 range (Park et al. 2012). Experimental work confirms that the IPGE and Rh partition into chromite with partition coefficients in the range 40 to 200 at $f\text{O}_2$ around Ni–NiO and at higher $f\text{O}_2$, the values can approach 1000 (Brenan et al. 2012; Righter et al. 2004).

Collection of the IPGE and Rh by chromite would better explain the tendency of the chromite layers to show peak mantle-normalized concentrations at Rh rather than Ru. A comparison of the metal patterns of chromite from the Bushveld chilled margins (Pagé and Barnes 2013) shows many similarities with the G-chromite layer (Fig. 18a). Assuming that the G chromite layers do not contain any added sulfide component and that the PGE content of the magma is similar to the B-1 magma, we can also calculate the partition

coefficients required to produce the G layer chromites as 44 for Ir, 32 for Rh, and 115 for Ru (ESM 8), which are similar to the experimental determined partition coefficients. On the plots of IPGE and Rh vs Cr_2O_3 (Fig. 12), the samples, in part, plot along mixing lines between this theoretical chromite and the B-1 magma. Some samples, containing less than 1 % Cr_2O_3 , plot below the mixing line possibly because of the dilution effect of the silicate cumulate minerals. Some samples plot above the mixing line, possibly these samples contain a sulfide component.

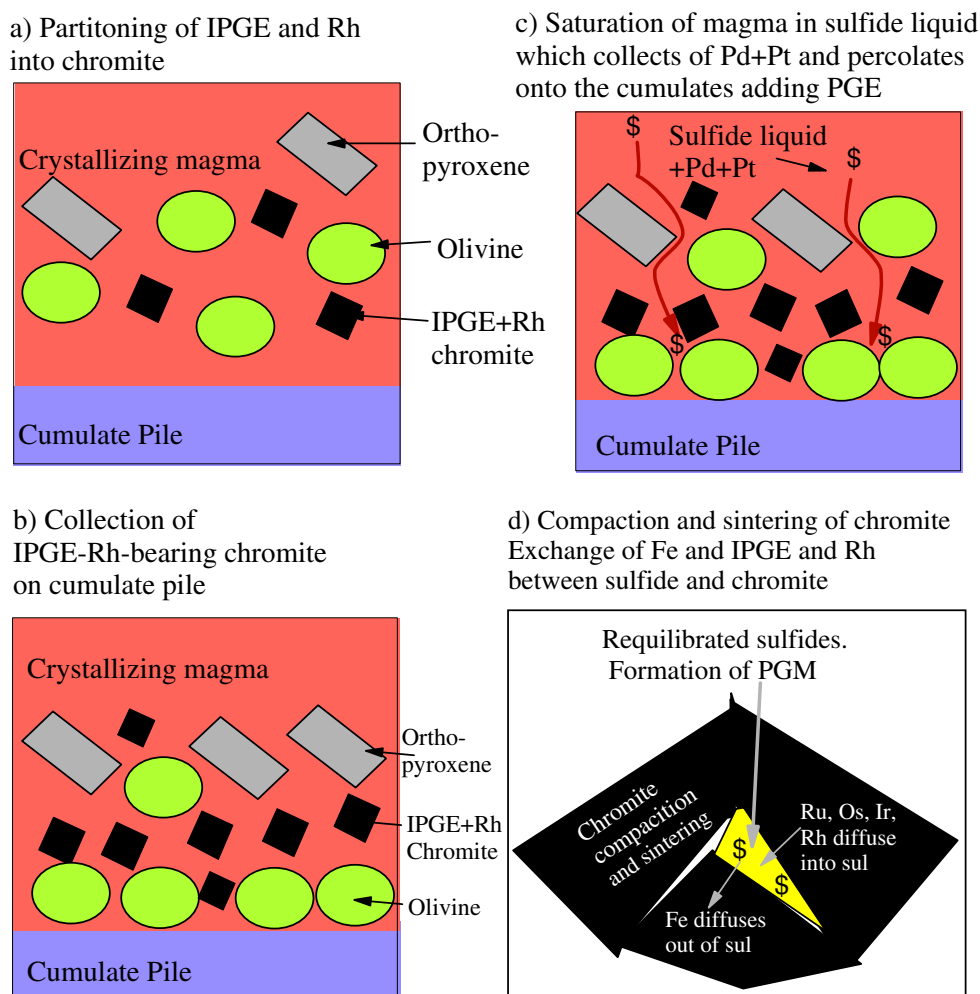
If the IPGE and Rh were originally collected by chromite, how did these elements now come to be present in laurite and base metal sulfides? We suggest that IPGE and Rh partitioned into chromite from a magma that was not yet saturated in a base metal sulfide liquid and the chromite collected on the cumulate pile (Fig. 19a, b). The magma later became saturated in base metal sulfide liquid, and Cu, Pd, Se and the remaining PGE partitioned into the base metal sulfide liquid which settled onto the cumulus pile among the chromite grains (Fig. 19c), much as described in the PGM collection model.

Chromite has undergone post-cumulus growth and recrystallization. Evidence for sub-solidus growth of chromites is provided by the triple junctions between chromites of the chromite layers (Fig. 3e) and a crystal size distribution study of some chromite layers (Waters and Boudreau 1996). During this growth, some interstitial material including sulfide minerals was enclosed by the chromite grains (Fig. 19d). The PGE that was present in the chromite could have diffused into the sulfide minerals by exchange of Fe and PGE between the sulfide and the chromite (Fig. 19d). Ruthenium would have been the PGE that was present in the greatest abundance in chromite, and thus, the most common PGM that formed from the base metal sulfide was laurite. Much of the Os and Ir and some of the Rh from the chromite diffused into laurite. The Rh that could not be accommodated in laurite diffused into the base metal sulfides. The loss of the Fe from the sulfide minerals resulted in the base metal sulfides now consisting mainly of Ni and Cu sulfides.

We can estimate the volume of chromite required to make one laurite grain of $5 \mu\text{m}^3$ as 0.64 mm^3 , assuming that the chromite originally contained 300 ppb Ru [similar to the value found in most chromite phenocrysts (Park et al. 2012; Pagé and Barnes 2013)] and assuming that the laurite contained 50 % Ru.

The Bushveld and Great Dyke chromite layers show peaks at Ru in the lower chromite layers (Figs. 10 and 11). The lower chromite layers in both of intrusions have patterns similar to the chromite from the Bushveld chills. To explain the shift in the peak of the patterns to Rh in the middle chromites, we argue that a little base metal sulfide was added. The peak in the patterns moves to Rh because sulfides add more Rh than IPGE, but not enough Pt and Pd to overcome the effect of Rh

Fig. 19 Model for collection of IPGE and Rh by chromite followed by saturation of the magma in a base metal sulfide liquid which collected Pd, Cu, and Se followed inclusion of base metal sulfides in chromite during cooling and exchange of between chromite and sulfides of Fe and IPGE and Rh



in the chromite. In the upper chromite layers, there has been a larger addition of a metal sulfide liquid component, and hence, the peak moves to Pt and Pd.

A weakness of this model is that the diffusion coefficients for the IPGE and Rh from chromite to sulfides are unknown, and thus, whether diffusion of the IPGE and Rh is possible is unknown at present.

Summary and conclusions

Like the ultramafic rocks of the Bushveld Complex and Great Dyke, the Ultramafic series of the Stillwater Complex show enrichment in all the PGE. The chromite layers show the greatest degrees of enrichment with preferential enrichment in IPGE and Rh over Pt and Pd.

The most common PGM present is laurite, which hosts most of the Ru and, to a lesser extent, the Os and Ir in the rocks. The base metal sulfides are mainly pentlandite, chalcopyrite, millerite, and bornite. Preliminary analyses show that they are rich in Pd and Rh and are probably the main host for

these elements. The major carrier of Pt is assumed to be the μm -sized Pt minerals associated with the base metal sulfides.

The S content of all of the rocks is very low—in most cases <100 ppm—which would normally be considered too low for the PGE to have been collected by a base metal sulfide liquid. However, the S/Se ratios of many of the rocks are very low (<1500), which combined with the textural observations, suggesting that rocks have lost much of their original S; thus, collection of the PGE by a base metal sulfide liquid followed by S loss could have occurred.

However, collection of PGE by a base metal sulfide liquid will not account for the preferential enrichment of IPGE and Rh in the chromite layers. One possible model to account for this is that as the intrusion cooled a hydromagmatic fluid dissolved much of the sulfide and preferentially re-mobilized Pd and some Pt from the layers. As a result of S loss, laurite and other PGM exsolved from sulfides. The laurite and other PGM were then included in the chromite during post-cumulus growth. Because Pd, Cu, and Se correlate with each other for this model to be viable, Se must be mobilized along with Pd and Cu. The weakness of this model is there is not

sufficient experimental data to say with any certainty whether a magmatic fluid could transport Pd and Pt.

The classic model of crystallization of laurite (which collected the IPGE) and chromite together, followed by addition of a Pd–Pt–Rh bearing base metal sulfide liquid to the cumulate pile followed by S loss was considered. This model satisfies the IPGE distribution, but will not account for the enrichment of Rh relative to Pd and Pt on most the mantle normalized patterns. It also does not explain why Rh shows a positive correlation with Cr₂O₃ and does not show a positive correlation with Se.

Experimental work has shown that IPGE and Rh partition into chromite, and IPGE and Rh are homogeneously distributed in chromite phenocrysts from volcanic rocks and chromites from the Bushveld marginal sills. We suggest that at Stillwater, the IPGE and Rh partitioned into chromite. The Pd and the balance the PGE were added by base metal sulfide liquid. During post-cumulus sintering of the chromite grains, some the base metal sulfide grains were included in the chromite. The Fe in the sulfide and PGE in the chromite exchanged resulting in the replacement of pyrrhotite by laurite and enrichment of Rh in the residual base metal sulfide. Subsequently, many of the samples lost some S either during metamorphism or late magmatic processes. In this model, the shape of the PGE patterns are the result of mixing of chromite rich in IPGE, Rh, and Pd–Pt-bearing base metal sulfide liquid.

Acknowledgments We would like to thank Mr. Dany Savard and Ms. Sahdi Mehdi for their careful analytical work. The reviewers, Prof. Alan Boudreau Dr. Steve Barnes and Dr. M. Fiorentini are thanked for their detailed reviews. This work was funded by a Canadian Natural Science and Engineering Research Council Discovery Grant to SJB (17313) and a Canada Research Chair program grant to SJB (215503).

Conflict of interest The authors declare that they have no conflict of interest.

References

- Aird HM, Boudreau AE (2013) High-temperature carbonate minerals in the Stillwater Complex, Montana, USA. *Contrib Mineral Petrol* 166: 1143–1160
- Ballhaus C, Ryan CG, Memagh TP, Green DH (1994) The partitioning of Fe, Ni, Cu, Pt and Au between sulfide, metal, and fluid phases: a pilot study. *Geochim Cosmochim Acta* 57:811–826
- Barnes S-J, Maier WD (2002) Platinum-group element distributions in the Rustenburg Layered Suite of the Bushveld Complex, South Africa. In: Cabri LJ (ed) *The geology, geochemistry, mineralogy and mineral beneficiation of platinum-group elements*. Can Institute of Mining, Metallurgy and Petroleum Spec. vol. 54. p. 553–580
- Barnes S-J, Boyd R, Komelliussen A, Nilssen L-P, Often M, Pedersen R-B, Robins B (1988) The use of mantle normalization and metal ratios in discriminating the effects of partial melting, crystal fractionation and segregation on platinum group elements, gold, nickel and copper: examples from Norway. In: Prichard HM, Potts PJ, Bowles JFW, Cribb SJ (eds) *Geoplatinum 87*. Elsevier, London, pp 113–143
- Barnes S-J, Savard D, Bédard LP, Maier WD (2009) Selenium and sulfur concentrations in the Bushveld Complex of South Africa and implications for formation of the platinum-group element deposits. *Miner Deposita* 44:647–663
- Barnes S-J, Maier WD, Curl EA (2010) Composition of the marginal rocks and sills of the Rustenburg Layered Suite, Bushveld Complex, South Africa: implications for the formation of the platinum-group element deposits. *Econ Geol* 105:1491–1511
- Bazarkina EF, Pokrovski GS, Hazemann J-L (2014) Structure, stability and geochemical role of palladium chloride complexes in hydrothermal fluids. *Geochim Cosmochim Acta* 146:107–131
- Bédard LP, Barnes S-J (2002) A comparison of N-type semi-planar and coaxial INAA detectors for 33 geochemical reference samples. *J Radioanal Nucl Chem* 254:485–497
- Bédard LP, Savard D, Barnes S-J (2008) Total sulfur concentrations in geological reference materials by elemental infrared analyser. *Geostand Geoanal Res* 32:203–208
- Blaine FA, Linnen RL, Holtz F, Brüggemann GE (2005) Platinum solubility in a haplobasaltic melt at 1250 C and 0.2 GPa: the effect of water content and oxygen fugacity. *Geochim Cosmochim Acta* 69:1265–1273
- Borisov A (2005) Crystallization and stability of noble metal alloys in the magmatic process. *Geol Ore Deposits* 47:469–475
- Boudreau A, McCallum I (1989) Investigations of the Stillwater Complex: part V. Apatites as indicators of evolving fluid composition. *Contrib Mineral Petrol* 102:138–153
- Boudreau AE, Mathez EA, McCallum IS (1986) Halogen geochemistry of the Stillwater and Bushveld Complexes: evidence for transport of the platinum-group elements by Cl-rich fluids. *J Petrol* 27:967–986
- Brenan JM, Andrews D (2001) High temperature stability of laurite and Ru–Os–Ir alloy and their role in PGE fractionation in mafic magmas. *Can Mineral* 39:341–360
- Brenan JM, Finnigan CF, McDonough WF, Homolova V (2012) Experimental constraints on the partitioning of Ru, Rh, Ir, Pt and Pd between chromite and silicate melt: the importance of ferric iron. *Chem Geol* 302:16–32
- Butler JR (1966) Geologic evolution of the Beartooth Mountains, Montana and Wyoming. Part 6. Cathedral Peak Area, Montana. *Geol Soc Am Bull* 77:45–64
- Cooper RW (1997) Magmatic unconformities and stratigraphic relations in the Peridotite zone, Stillwater Complex, Montana. *Can J Earth Sci* 34:407–425
- Cooper R, Garuti G, Zaccarini F (2005) Platinum group minerals distribution in chromite layers of the Stillwater complex (Montana, USA). In: Törmänen T, Alapieti TT (eds) *10th International Platinum Symposium*. Geological Survey Finland, Oulu, pp 58–61
- Crockett JH, Fleet ME (1997) Implications of composition for experimental partitioning of platinum-group elements and gold between sulfide liquid and basalt melt: the significance of nickel content. *Geochim Cosmochim Acta* 61:4139–4149
- Djon MLN, Barnes S-J (2012) Changes in sulfides and platinum-group minerals with the degree of alteration in the Roby, Twilight, and High Grade Zones of the Lac des Iles Complex, Ontario, Canada. *Miner Deposita* 47:1–22
- Ertel W, O'Neill HSC, Sylvester P, Dingwell D (1999) Solubilities of Pt and Rh in a haplobasaltic silicate melt at 1300 C. *Geochim Cosmochim Acta* 63:2439–2449
- Finnigan CS, Brenan JM, Mungall JE, McDonough WF (2008) Experiments and models bearing on the role of chromite as a collector of platinum group minerals by local reduction. *J Petrol* 49: 1647–1665
- Fortenfant SS, Günther D, Dingwell DB, Rubie DC (2003) Temperature dependence of Pt and Rh solubilities in a haplobasaltic melt. *Geochim Cosmochim Acta* 67:123–131

- Garuti G, Proenza J, Zaccarini F (2007) Distribution and mineralogy of platinum-group elements in altered chromitites of the Campo Formoso layered intrusion (Bahia State, Brazil): control by magmatic and hydrothermal processes. *Mineral Petrol* 89:159–188
- Godel B (2013) High-resolution X-ray computed tomography and its application to ore deposits: from data acquisition to quantitative three-dimensional measurements with case studies from Ni-Cu-PGE deposits. *Econ Geol* 108:2005–2019
- Godel B, Barnes S-J (2008) Platinum-group elements in sulfide minerals and the whole rock of the J-M Reef (Stillwater complex): implication for the formation of the reef. *Chem Geol* 248:272–294
- González-Jiménez JM, Griffin WL, Gervilla F, Proenza JA, O'Reilly SY, Pearson NJ (2013) Chromitites in ophiolites: How, where, when, why? Part I. A review and new ideas on the origin and significance of platinum-group minerals. *Lithos* 189:127–139
- Gornostayev SS, Laajoki K, Leinonen O (2000) The platinum-group minerals in the Kemi chromite deposit, Finland: a case study of the Eljävärvi ore body. In: GEODE-Fennoscandian Shield Workshop, Gällivare-Kiruna, Sweden, vol 6. p 16–22
- Hanley JJ, Mungall JE, Pettke T, Spooner ETC, Bray CJ (2008) Fluid and halide melt inclusions of magmatic origin in the Ultramafic and Lower Banded Series, Stillwater Complex, Montana, USA. *J Petrol* 49:1133–1160
- Hiemstra S (1979) The role of collectors in the formation of the platinum deposits in the Bushveld Complex. *Can Mineral* 17:469–482
- Junge M, Oberthür T, Melcher F (2014) Cryptic variation of chromite chemistry, platinum group element and platinum group mineral distribution in the UG-2 chromite: an example from the Karee Mine, Western Bushveld Complex, South Africa. *Econ Geol* 109:795–810
- Kanitpanyacharoen W, Boudreau A (2013) Sulfide-associated mineral assemblages in the Bushveld Complex, South Africa: platinum-group element enrichment by vapor refining by chloride-carbonate fluids. *Miner Deposita* 48:193–210
- Keays RR, Lightfoot PC, Hamlyn PR (2012) Sulfide saturation history of the Stillwater Complex, Montana: chemostratigraphic variation in platinum group elements. *Miner Deposita* 47:151–173
- Kinloch ED (1982) Regional trends in the platinum-group mineralogy of the Critical Zone of the Bushveld Complex, South Africa. *Econ Geol* 77:1328–1347
- Laurenz V, Fonseca RO, Ballhaus C, Jochum KP, Heuser A, Sylvester PJ (2013) The solubility of palladium and ruthenium in picritic melts: 2. The effect of sulfur. *Geochim Cosmochim Acta* 108:172–183
- Li C, Ripley EM, Merino E, Maier WD (2004) Replacement of base metal sulfides by actinolite, epidote, calcite and magnetite in the UG2 and Merensky Reef of the Bushveld Complex, South Africa. *Econ Geol* 99:173–184
- Locmelis M, Pearson NJ, Barnes SJ, Fiorentini ML (2011) Ruthenium in komatiitic chromite. *Geochim Cosmochim Acta* 75:3645–3661
- Maier WD, Prichard HM, Barnes SJ, Fisher PC (1999) Compositional variation of laurite at Union Section in the Western Bushveld Complex. *S Afr J Geol* 102:286–292
- Maier WD, Barnes S-J, Groves D (2013) The Bushveld Complex, South Africa: formation of platinum-palladium, chrome-and vanadium-rich layers via hydrodynamic sorting of a mobilized cumulate slurry in a large, relatively slowly cooling subsiding magma chamber. *Miner Deposita* 48:1–56
- McCallum IS (2002). The Stillwater Complex: a review of the geology. In: 9th International Platinum Symposium, Geology and Guide Stillwater Complex, Montana, USA, Billings. p 21–25
- McCallum IS, Raedeke LD, Mathez ED (1980) Investigations of the Stillwater Complex: Part I. Stratigraphy and structure of the Banded zone. *Am J Sci* 280:59–87
- McDonough WF, Sun S-S (1995) The composition of the Earth. *Chem Geol* 120:223–253
- Merkle RKW (1992) Platinum-group minerals in the middle group of chromitite layers at Marikana, western Bushveld Complex: indications for collection mechanisms and postmagmatic modification. *Can J Earth Sci* 29:209–221
- Mungall J, Brennan J (2014) Partitioning of platinum-group elements and Au between sulfide liquid and basalt and the origins of mantle-crust fractionation of the chalcophile elements. *Geochim Cosmochim Acta* 125:265–289
- Naldrett AJ (2011) Fundamentals of magmatic sulfide deposit. In: Li C, Ripley EM (eds) Magmatic Ni-Cu and PGE deposits: geology, geochemistry, and genesis, reviews in economic geology, vol 17. Society of Economic Geologists, Lillteton, pp 1–50
- Naldrett A, Lehmann J (1988) Spinel non-stoichiometry as the explanation for Ni-, Cu- and PGE-enriched sulphides in chromitites. In: Prichard HM, Potts PJ, Bowles JFW, Cribb SJ (eds) *Geoplatinum* 87. Elsevier, London, pp 93–109
- Naldrett AJ, Kinnaird J, Wilson A, Yudovskaya M, McQuade S, Chunnnet G, Stanley C (2009) Chromite composition and PGE content of Bushveld chromitites: part 1—the Lower and Middle Groups. *Appl Earth Sci: Trans Inst Min Metall Sect B* 118:131–161
- Oberthür T (2002). Platinum-group element mineralization of the Great Dyke, Zimbabwe. In: Cabri LJ (ed) *The geology, geochemistry, mineralogy and mineral beneficiation of platinum-group elements*. *Can Inst Min, Metall Petrol Special* vol 54. p 483–506
- Ohnenstetter D, Watkinson DH, Jones PC, Talkington RW (1986) Cryptic compositional variation in laurite and enclosing chromite from the Bird River Sill, Manitoba. *Econ Geol* 81:1159–1168
- Page NJ (1971) Sulfide minerals in the G and H chromitite zones of the Stillwater Complex, Montana. U.S Geological Survey Professional Paper 694: 20 p
- Page NJ (1977) Stillwater Complex, Montana: rock succession, metamorphism and structure of the complex and adjacent rocks. U.S Geological Survey Professional Paper 999: 79 p
- Pagé P, Barnes S-J (2013) Improved in-situ determination of PGE concentration of chromite by LA-ICP-MS: Towards a better understanding. In: *Mineral Deposit research for a high-tech world, 12th Biennial SGA Meeting, Uppsala*, p 1050–1053
- Pagé P, Barnes S-J, Bédard JH, Zientek ML (2012) In situ determination of Os, Ir, and Ru in chromites formed from komatiite, tholeiite and boninite magmas: implications for chromite control of Os, Ir and Ru during partial melting and crystal fractionation. *Chem Geol* 302:3–15
- Park J-W, Campbell IH, Eggins SM (2012) Enrichment of Rh, Ru, Ir and Os in Cr spinels from oxidized magmas: evidence from the Ambae volcano, Vanuatu. *Geochim Cosmochim Acta* 78:28–50
- Patten C, Barnes S-J, Mathez EA (2012) Textural variations in MORB sulfide droplets due to differences in crystallization history. *Can Mineral* 50:675–692
- Patten C, Barnes S-J, Mathez EA, Jenner FE (2013) Partition coefficients of chalcophile elements between sulfide and silicate melts and the early crystallization history of sulfide liquid: LA-ICP-MS analysis of MORB sulfide droplets. *Chem Geol* 358:170–188
- Peach CL, Mathez EA, Keays RR (1990) Sulfide melt-silicate melt distribution coefficients for noble metals and other chalcophile elements as deduced from MORB: implications for partial melting. *Geochim Cosmochim Acta* 54:3379–3389
- Peregodova A, Barnes S-J, Baker DR (2006) An experimental study of mass transfer of platinum-group elements, gold, nickel and copper in sulfur-dominated vapor at magmatic temperatures. *Chem Geol* 235: 59–75
- Potts PJ (1987) *A handbook of silicate rock analysis*. Blackie Glasgow
- Prichard HM, Neary C, Fisher PC, O'Hara M (2008) PGE-rich podiform chromitites in the Al 'Ays Ophiolite Complex, Saudi Arabia: an example of critical mantle melting to extract and concentrate PGE. *Econ Geol* 103:1507–1529
- Prichard H M, Barnes S-J, Fisher P C, Pagé P, Zientek M (2014) PGM in the Stillwater chromitites and implications for the magmatic

- processes that formed the ultramafic part of the Stillwater Complex. XII International Pt Symposium, Yekaterinburg, Russia
- Righter K, Campbell AJ, Humayun M, Hervig RL (2004) Partitioning of Ru, Rh, Pd, Ir and Au between Cr-bearing spinel, olivine, pyroxene and silicate melts. *Geochim Cosmochim Acta* 68:867–880
- Savard D, Bédard LP, Barnes S-J (2006) TCF selenium preconcentration in geological materials for determination at sub micro-gm with INAA (Se TCF/INAA). *Talanta* 70:566–571
- Savard D, Barnes SJ, Meisel T (2010) Comparison between nickel-sulfur fire assay Te co-precipitation and isotope dilution with high-pressure asher acid digestion for the determination of platinum-group elements, rhenium and gold. *Geostand Geoanal Res* 34:281–291
- Scoon RN, Teigler B (1994) Platinum-group element mineralization in the critical zone of the Western Bushveld Complex: 1. Sulfide poor chromitites below the UG2. *Econ Geol* 89:1094–1121
- Smith JW, Holwell DA, McDonald I (2014) Precious and base metal geochemistry and mineralogy of the Grasvally Norite–Pyroxenite–Anorthosite (GNPA) member, northern Bushveld Complex, South Africa: implications for a multistage emplacement. *Miner Deposita* 49:667–692
- Tagirov BR, Baranova NN, Zotov AV, Akinfiyev NN, Polotnyanko NA, Shikina ND, Koroleva LA, Shvarov YV, Bastrakov EN (2013) The speciation and transport of palladium in hydrothermal fluids. Experimental modeling and thermodynamic constraints. *Geochim Cosmochim Acta* 117:348–373
- Talkington RW, Lipin BR (1986) Platinum-group minerals in chromite seams of the Stillwater Complex, Montana. *Econ Geol* 81:1179–1186
- Thomson JA (2008) Beneath the Stillwater Complex: Petrology and geochemistry of quartz-plagioclase-cordierite (or garnet)-orthopyroxene-biotite±spinel hornfels, Mountain View area, Montana. *Am Mineral* 93:438–450
- Todd SG, Keith DW, LeRoy LW, Shissel DJ, Mann EL, Irvine TN (1982) The J-M platinum-palladium Reef of the Stillwater Complex, Montana: I. Stratigraphy and petrology. *Econ Geol* 77:1454–1480
- Von Gruenewaldt G, Hatton CJ, Merkle RKW, Gain SB (1986) Platinum-group element-chromite associations in the Bushveld Complex. *Econ Geol* 81:1067–1079
- Wall CJ, Scoates JS, Friedman RM, Weis DA, Meurer W (2010) Baddeleyite-Zircon Relationships in cumulates of the Archean Stillwater Complex: evidence from U-Pb geochronology and Hf isotope systematics. *AGU Fall Meeting Abstracts* p 2309
- Waters C, Boudreau AE (1996) A re-evaluation of crystal-size distributions in chromite cumulates. *Am Mineral* 81:1452–1459
- Webb PC, Thompson M, Potts PJ, Bédard LP (2006) GEOPT18—an international proficiency test for analytical geochemistry laboratories—report on round 18/Jan 2006 (Quartz diorite, KPT-1). International Association of Geoanalysts. www.geoanalyst.org/geopt/GeoPT18Report.pdf accessed 12 June 2014
- Wooden JL, Czamanske GK, Zientek ML (1991) A lead isotopic study of the Stillwater Complex Montana; constraints on crustal contamination and source regions. *Contrib Mineral Petrol* 107:80–93
- Zientek ML (2012) Magmatic ore deposits in layered intrusions—descriptive model for reef-type PGE and contact-type Cu-Ni-PGE deposits. U.S Geological Survey Open File 2012–1010. p 48
- Zientek ML, Foose MP, Mei L (1986) Palladium, platinum, and rhodium contents of rocks near the lower margin of the Stillwater Complex, Montana. *Econ Geol* 81:1169–1178
- Zientek ML, Cooper RW, Corson SR, Geraghty EP (2002) Platinum-group element mineralization in the Stillwater Complex, Montana. In: Cabri, LJ (ed) *Geology, geochemistry, mineralogy and mineral beneficiation of platinum group element*. *Can Inst Min Metall Petrol Spec* vol 54. p 459–481